Southern Hemisphere $u'g'r'i'z'$ Standard Stars

J. Allyn Smith[1,2,3,4,6], Sahar S. Allam[1,5,4,7], Douglas L. Tucker[5,4,8], Justin L. Stute[1,2], Christopher T. Rodgers[1,4,9], and Chris Stoughton[5,4,10]

Received ______________; accepted ______________

November 27, 2006

[1]University of Wyoming, Department of Physics & Astronomy, Laramie, WY 82071

[2]Los Alamos National Laboratory, ISR-4, D448, Los Alamos, NM 87545

[3]Current Address: Department of Physics & Astronomy, Austin Peay State University, P.O. Box 4608, Clarksville, TN 37044

[4]Visiting Astronomer, Cerro Tololo Inter-American Observatory. CTIO is operated by AURA, Inc. under contract to the National Science Foundation.

[5]Fermi National Accelerator Laboratory, P.O. Box 500, Batavia, IL 60510

[6]smithj@apsu.edu

[7]sallam@fnal.gov

[8]dtucker@fnal.gov

[9]crodgers@uwyo.edu

[10]stoughto@fnal.gov

ABSTRACT

We present 16,003 southern hemisphere stars in 58 fields for use as standards in the $u'g'r'i'z'$ photometric system. These stars extend the original standard star network developed for the Sloan Digital Sky Survey to a complete all-sky network. These additional stars also extend the existing standard system to fainter magnitudes ($r' = 9.2 - 18.2$) and a wider color range ($-1.0 < g' - r' < 2.8$). We describe changes to the reduction method and software which have been incorporated since the original program, and we provide site extinction coefficients for Cerro Tololo Interamerican Observatory (CTIO) over the 5 year period of 2000–2004.

Subject headings: catalogs — stars: fundamental parameters — standards

1. Introduction

The photometric calibration of the Sloan Digital Sky Survey (SDSS) is based on the five-filter, wide-band photometric system ($u'g'r'i'z'$) defined by Fukugita et al. (1996). This system offers three distinct astrophysical advantages over the established Johnson-Cousins $UBVRI$ system: 1) sharper cutoffs of the band edges, 2) minimal overlap of spectral regions between filters, and 3) filter breaks chosen to exclude the strongest night sky emission lines. We note the SDSS z' filter is open on the red end. Therefore, the system transformation coefficients for z' band are strongly dependent upon the choice of detector that observers use to match the standard star network.

Fukugita et al. (1996) presented the $u'g'r'i'z'$ filter system which now forms the basis of the Sloan Digital Sky Survey (SDSS) imaging program (Gunn et al. 1998). Smith et al. (2002) developed the original 158 primary standard stars which defined the $u'g'r'i'z'$

photometric system using the 1m telescope at the U.S. Naval Observatory, Flagstaff Station. These stars, in northern and equatorial regions, form the basis for the photometric calibration of the SDSS (York et al. 2000; Hogg et al. 2001; Ivezić et al. 2004, 2007; Gunn et al. 2006; Tucker et al. 2006). The defining instrument system and filters, the observing process, the reduction techniques, and the software used to create the initial stellar network were all described in Smith et al. (2002).

However, the original set of standard stars is essentially a northern hemisphere and equatorial network. As such, it is of limited value to observers in the southern hemisphere. For the $u'g'r'i'z'$ filter system to become widely accepted, southern hemisphere standard stars are needed. Additional ground-based projects which plan to use some or all of the SDSS filters (e.g. DES, LSST, VSS, OmegaCam) will be located in the southern hemisphere or near the equator to study large fractions of the southern hemisphere. Therefore, we undertook the natural project, as part of the NOAO Surveys Program[11], to extend the $u'g'r'i'z'$ standards into the southern hemisphere. These new standards are tied to the existing northern network via the equatorial standard stars (Smith et al. 2002) developed to support the SDSS (York et al. 2000). The first results of the southern efforts were presented in Smith et al. (2003) and we now present the completed initial (v1.0) southern $u'g'r'i'z'$ standard network. As discussed later on, updates to the system will be posted as available on our web site at `http://www-star.fnal.gov`.

To fully understand the $u'g'r'i'z'$ standard star development, one must understand the early history of the SDSS (Smith et al. 2007). The primary goals for the original SDSS were large scale structure studies using galaxies ($z < 0.4$) and QSOs. Therefore, the first version of the standard network was limited, for the most part, to stars bluer than about M0 to avoid the strengthening metal bands and flare stars. Further, most of the survey area (up

[11] `http://www.noao.edu/gateway/surveys/programs.html`

to ∼9,000 square deg.) is centered on the North Galactic Pole with a smaller area along the celestial equator. Because of this, a heavy emphasis was placed on northern hemisphere stars during the development of the primary standard network. Additional stars near the celestial equator were selected from other standard works (i.e. Landolt 1973, 1983a, 1992). In this work, these equatorial stars are used to tie the southern hemisphere extension to the original northern network. The use of existing standards also allows us to shorten the time required to develop the original set of $u'g'r'i'z'$ network as most variables in these pre-existing standard fields have been identified. This practice was continued in this work due to the limited telescope time allocated for the project — 84 nights spread over four years — versus the 183 nights over two years (and growing again, see § 5) used to develop the northern network.

One of the goals of the SDSS was to achieve a level of photometric uniformity and accuracy such that the system-wide rms errors in the final SDSS photometric catalog would be less than 0.02 mag in r', 0.02 mag in $(r' - i')$ and $(g' - r')$, and 0.03 mag in $(u' - g')$ and $(i' - z')$, for objects bluer than an M0 dwarf. To meet this target, internal goals were set for the minimum precision accuracy of the primary standard star system: the uncertainty in the mean calibrated magnitudes for any given primary standard star needed to be ≤1.5% at u', ≤ 1% in g', r' and i', and ≤1.5% at z'. We attempted to maintain these same levels for the secondary standards presented here, though the CCD-based observing program used exposure times tailored for selected stars in some fields. The result is that some of the fainter stars in these fields suffer from a low signal-to-noise. However, as discussed in § 4 we employ a S/N cut in the current work to minimize "noisy" stars.

One of the major drawbacks of the original (northern) standard star network was the use of bright stars. This was dictated by the necessity of using an 0.5m photometric monitoring telescope (PT) in the SDSS. The planned strategy of the SDSS called for the

PT to observe five to six standard stars and two fainter secondary patches in the survey area each hour (York et al. 2000; Tucker et al. 2006). In order to accommodate larger telescopes, the southern extension includes fainter stars.

As discussed in Smith et al. (2002), the $u'g'r'i'z'$ system uses the F subdwarf BD+17°4708 to set the initial system zeropoint (our "fundamental" standard) with the other 157 stars of the system being referred to as "primary" standards. BD+17°4708 has direct spectrophotometry with respect to Vega. The term "secondary" is used within the SDSS nomenclature to refer to the photometric system transfer patches — pieces of the sky that are observed by the 0.5m PT that are used to transfer the photometric solution to the main survey imaging telescope (Tucker et al. 2006). The stars presented in this paper are intended as secondary standards in the more traditional sense. That is, their magnitudes and colors are derived from the primary system standards and are intended for use as calibration stars for other observations. As such, they extend the existing primary system to fainter magnitudes and a wider color range. As a further note, we point out that the $u'g'r'i'z'$ network is an AB magnitude system (Oke & Gunn 1983), not a Vega magnitude system.

In the following sections we present details of the southern $u'g'r'i'z'$ standard star program. We describe the instrumentation and filter system, the candidate selection strategy, and the observing strategy in § 2. We present our data reduction methodology in § 3. Final results for the initial set of southern $u'g'r'i'z'$ secondary standard stars are presented in § 4, and a discussion of planned future enhancements to the overall system is presented in § 5.

2. Observations

The data for this project were collected during 84 nights split into 12 observing runs, each typically a week long. These were conducted over a four year period between September 2000 and May 2004. The "Journal of Observations" is presented in Table 1 and lists the circumstances of our observing runs. The first three columns give the year and month, the UT dates, and the Modified Julian Dates (MJD)[12] of each observing run; the fourth and fifth columns give the number of nights allocated for each observing run and the number judged to be clear in whole or in part (more than two hours at a stretch) by the observers; and the sixth column gives the number of observations obtained during the "clear" portion of the run. Of the 84 nights allocated for this project, 49 were judged to be clear by the observer and were used to calibrate the new southern standard stars.

EDITOR: PLACE TABLE 1 HERE.

2.1. Instrumentation

We used the CTIO 0.9-m telescope equipped with the Tek2k#3 CCD operating at the cassegrain focus. This "Grade-1" CCD is thinned and has an anti-reflection coating, resulting in high quantum efficiency similar to that of the detector used to establish the initial standard star system[13]. Observers have used this CCD in a stable configuration on this telescope since October 1995. The imager was controlled by the CTIO Arcon software (version 3.3) and operated in multiple (quad) amplifier read mode. The average gain and

[12]The Modified Julian Date is defined by the relation MJD $\equiv$ JD $-$ 2400000.5, where JD is the Julian Date.

[13]`http://www.ctio.noao.edu/ccd_info/ccd_info.html`

read noise values used in this project are listed in Table 2 for each of the four amplifiers. The CCD has 24μ pixels which yields a scale of 0.396 arcsec/pixel and results in a 13.5 arc-minute field of view. We observed with the CTIO SDSS $u'g'r'i'z'$ filter set.

EDITOR: PLACE TABLE 2 HERE.

We have generated preliminary response functions for the CTIO-0.9m+Tek2k#3+$u'g'r'i'z'$ filter system based upon the $u'g'r'i'z'$ filter transmission curves from the manufacturer (Custom Scientific), and the CTIO Tek2k quantum efficiency from the GIF plot at the CTIO CCD Information website[14]. We assumed two aluminum reflecting surfaces from Bennett et al. (1963) as reproduced by Kneale (1994)[15]. Machine-readable tables of these preliminary filter responses are available at our public access URL[16], where updated versions will be posted as new data become available.

The filter plus detector response curves for both the CTIO-0.9m+Tek2k#3+$u'g'r'i'z'$ and, for comparison, those from the USNO-1.0m+Tek1k+$u'g'r'i'z'$ combination used to set up the original $u'g'r'i'z'$ standard star network are shown in Figure 1, reproduced from Figure 1 of Smith et al. (2003). The two system responses look quite similar and given the uncertainties in calculating the CTIO $u'g'r'i'z'$ response function, these curves are consistent with the results we report later in this paper (see § 3 below). The values for the instrumental color terms which we measure for the CTIO-0.9m data are typically quite small – ranging on average from about 0.03 to 0.05 mag per magnitude in color. (We must emphasize, though, that for the most accurate photometry — i.e., systematic errors less

[14] `http://www.ctio.noao.edu/ccd_info/ccd_info.html`

[15] `http://www.gemini.edu/documentation/webdocs/spe/spe-te-g0043.pdf`

[16] `http://www-star.fnal.gov`

than a few percent — the instrumental color terms must be solved for and applied when converting CTIO-0.9m $u'g'r'i'z'$ photometry to the USNO standard system.)

EDITOR: PLACE FIGURE 1 HERE.

We examined linearity of the CTIO system using the dome flat lamps on different observing runs and found the response to be stable, linear, and repeatable from 0− 60,000 DN. Seven tests were performed during five of the 12 observing runs over the four-year survey. Figure 2 shows the weighted average of the CCD response as a function of exposure time for two of these seven linearity sequences taken during the project (these were obtained during our 2002 September and 2003 July observing runs). Figure 3 shows the deviation from linearity by exposure time for the same data. Corresponding results from linearity tests obtained in our 2002 May observing run can be found in Figures 2 and 3 of Smith et al. (2003); we noticed no obvious changes in the this device's linearity response during the course of our project.

EDITOR: PLACE FIGURE 2 HERE.

EDITOR: PLACE FIGURE 3 HERE.

The supernovae monitoring group at CTIO made its shutter timing map available to us (N. Suntzeff, private communication), indicating expected deviations of $\leq 0.12\%$ (1.2 milli-mags) from center to edge of the CCD for our minimum exposure times of five seconds. Based on the shutter data obtained by this group, the shutter exposure timing is stable and repeatable.

2.2. Observing Strategy

We collected and median-combined calibration frames daily, usually during the afternoons. These consisted of a minimum of 10 bias (zero) and dome flat frames (10 per $g'r'i'z'$ filter). The dome flats were obtained with a color balance filter. Due to a lack of photons, we did not obtain u' dome flats. The dome flat images help us monitor the status of the CCD and look for changes in the flat-field structure. In addition, twilight sky flats were collected in all five filters during one or both of the twilight periods on each observable night. These were median-combined at the end of each observing run to produce a "master" twilight flat and used in the reduction of the data frames. We chose this approach to maintain consistency with the original standard network which made use of twilight flats only. At some point during most observing runs, we also collected long dark frames to monitor changes in the hot pixel pattern on the CCD and to look for light leaks. We also generated fringe correction frames for each run using the long program object exposures and/or targeted exposures of sparsely populated fields. These were applied to the i' and z' band images.

During a typical night in our standards program, we observed five or six existing standard fields three times — at the start, near the middle, and at the end of the night — in order to establish an extinction and color term baseline. Between these extended standard sequences, we usually alternated one to three program fields and one to three standard fields at different airmasses. We used these to monitor the extinction values and changes in the night sky conditions established by the longer extinction scans. This observing method allows us to maximize the number of target fields while continuously monitoring the atmosphere for changes. Exposure times for the established standard fields generally ranged from 5 to 200 seconds for typical $1''$ seeing: some u exposures were longer.

The program observations — performed during apparently clear conditions — consisted of one or two separate exposure cycles per candidate field, based on the magnitude range of stars of interest in each field. During non-photometric, but observable weather, we would hunt for additional field locations, monitor targets of opportunity, and obtain differential observations (generally r' band only) of the candidate fields for use in a differential search for variable stars. The long exposure cycles for some of the candidate fields allowed the observers to perform several visual checks of the sky to look for clouds and assess the general weather conditions.

Exposure lengths were tailored to maximize the number of potential standard stars in each field with good photon counts in all five filters while trying not to exceed the linear portion of the response curve for the primary star of interest. Tailoring the exposure lengths allowed us to develop multiple standards in several of the fields. However, the drawback of targeting the intended primary stars in each field is a decrease in the signal to noise for the extreme red or blue and fainter stars within the same field for which the exposures were not optimized.

At the end of each night, or the following day, we performed some fast quality checks to refine our feel for the night conditions. One check was to look at the archived IR satellite images to look for passing clouds and cloud trends. A second check was a review of the TASCA (Tololo All Sky CAmera) image loops each day to look for possible clouds, especially if any were noted of concern from the satellite maps. Though the TASCA is an optical camera and not very efficient when the moon was up, it readily shows clouds under dark conditions. Both the red and blue image loops were examined. Structures in the sky show easily in the red images and the blue images were used to sort the clouds from the night sky hydroxyl emissions, which show only in the red. We also examined the CTIO flux monitor output to look for dips associated with passing cloud. Though this monitor is uni-directional it does indicate if clouds are in the area of its monitor star. In addition, the general weather information (temperature, wind speed and direction, humidity) was examined to look for tell-tale trends of changing conditions. Finally, we would examine the La Silla weather to compare it to CTIO. Though the ESO site is several tens of kilometers north, it generally has similar weather.

2.3. Field Selection Strategy

Table 3 lists the field centers and typical exposure times for each of the filters, in seconds. The first column gives our internal field name, the right ascension and declination (J2000) for the center of the $13'$ field are given in columns two and three, and the typical exposure times (seconds) for each of the candidate fields for about $1''$ seeing are given in columns 4–8. Column 9 provides notes concerning the origin of the field. Several of the fields are taken from Landolt (1992) and are not marked as such. Those from Landolt (1992) with the note "Landolt - private communication" indicate that additional stars in those fields are in a forthcoming $UBVRI$ paper by Landolt. The existing northern standard star fields (Smith et al. 2002) which were used to tie the candidates to the existing network are listed in the top portion of the table and the final fields selected for the candidate southern standard stars are listed in the lower section of the table. Figure 4 shows the locations of the new southern standard fields and the existing northern and equatorial fields. The fields in common with Landolt's $UBVRI$ standards are shown in red.

EDITOR: PLACE TABLE 3 HERE.

EDITOR: PLACE FIGURE 4 HERE.

Our candidate field selection strategy for the southern hemisphere differed from the northern network. Based on discussions with several observers, and recognizing that most standard stars are too bright for the large telescopes, we devised a plan to make this system more "user friendly". The need for readily accessible standards to minimize slew times drove us to establish a grid of fields around the sky. We started by placing a field at each hour of right ascension at $-30°$ and $-60°$. In the final program, we reduced these fields to every other hour of right ascension to maximize the number of observations per field (we started with a goal of a minimum of 10 observations). These fields, together with the equatorial standards (Smith et al. 2002) establish the basic grid of stars. Next, we included fields in the E-regions, selecting patches from Graham (1982). We then moved/removed some fields which were too crowded.

To aid observers who want $u'g'r'i'z'$ and $UBVRI$ standards in the same area, we consulted with Landolt and included several of his $UBVRI$ fields which will be in one of his future works. We included a few fields near the Magellanic Clouds (Alvarado et al. 1995), in the South Galactic Cap (Graham 1981), and near the plane of the MW (Bok & Bok 1969). Finally, we included four special interest fields — the Chandra Deep Field South (see Smith et al. 2003) and three NOAO Deep Lens Survey fields (Tyson, private communication).

3. Reductions

3.1. `MTPIPE` Processing

We processed the raw data for this project using the SDSS software pipeline `MTPIPE`, an earlier version of which was used in the setup of the original $u'g'r'i'z'$ standard star network (Smith et al. 2002). `MTPIPE` is described in detail by Tucker et al. (2006). Briefly, this pipeline consists of four main packages:

- `preMtFrames`, which creates the directory structure for the reduction of a night's data, including parameter files needed as input for the other three packages, and runs quality-assurance tests on the raw data.

- `mtFrames`, which processes the images and performs object detection and aperture photometry on target field images. The processing steps include bias subtraction, flat-field and fringe-frame correction.

- `excal`, which takes the `mtFrames` aperture photometry lists for the Smith et al. (2002) standard star target fields, identifies the individual standard stars within those fields, and fits the observed raw counts and known $u'g'r'i'z'$ magnitudes to a set of photometric equations to obtain extinction, color term, and zero point coefficients.

- `kali`, which applies the fitted photometric equations to the `mtFrames` aperture photometry lists of program target fields for the appropriate analysis block.

For processing the data for the current paper, we used `MTPIPE` versions `v8.2` (`preMtFrames`, `mtFrames`, `excal`) and `v8.3` (`kali`), following the prescription described in § 3 of our previous southern $u'g'r'i'z'$ standards paper (Smith et al. 2003).

We note a few small differences between the methods employed in the current reductions and those used in setting up the original $u'g'r'i'z'$ standard star network of Smith et al. (2002). First, since we tailored our current effort toward calibrating standard stars which are typically much fainter than the Smith et al. (2002) standards (which were generally in the range $r' \approx 8 - 12$), we chose a smaller extraction size for our aperture photometry to reduce or minimize the background sky contribution to the noise. For the Smith et al. (2002) standards, we employed a 24″-diameter aperture in order to avoid problems associated with defocussing the brightest stars (required for some the observations). In the current program, we have chosen a 14.86″-diameter aperture. This smaller aperture reduces the effects of sky noise for the fainter target stars; as an added bonus, this size is used in the photometric calibration of the SDSS 2.5m data (Gunn et al. 1998; Lupton, Gunn &

Szalay 1999; York et al. 2000; Stoughton et al. 2002; Ivezić et al. 2004, 2007; Tucker et al. 2006). Tests on the fainter standards in Smith et al. (2002) show no significant deviations from the published magnitudes using this smaller extraction aperture.

Second, the current version of `MTPIPE` uses photometric equations which are slightly modified from the form described in §4.2 of Smith et al. (2002). The photometric equations employed in the current paper are the following:

$$\begin{aligned} u'_{\rm inst} &= u'_{\rm o} + a_u + k_u X \\ &\quad + b_u[(u'-g')_{\rm o} - (u'-g')_{\rm o,zp}] \\ &\quad + c_u[(u'-g')_{\rm o} - (u'-g')_{\rm o,zp}][X - X_{\rm zp}] , \end{aligned} \quad (1)$$

$$\begin{aligned} g'_{\rm inst} &= g'_{\rm o} + a_g + k_g X \\ &\quad + b_g[(g'-r')_{\rm o} - (g'-r')_{\rm o,zp}] \\ &\quad + c_g[(g'-r')_{\rm o} - (g'-r')_{\rm o,zp}][X - X_{\rm zp}] , \end{aligned} \quad (2)$$

$$\begin{aligned} r'_{\rm inst} &= r'_{\rm o} + a_r + k_r X \\ &\quad + b_r[(r'-i')_{\rm o} - (r'-i')_{\rm o,zp}] \\ &\quad + c_r[(r'-i')_{\rm o} - (r'-i')_{\rm o,zp}][X - X_{\rm zp}] , \end{aligned} \quad (3)$$

$$\begin{aligned} i'_{\rm inst} &= i'_{\rm o} + a_i + k_i X \\ &\quad + b_i[(i'-z')_{\rm o} - (i'-z')_{\rm o,zp}] \\ &\quad + c_i[(i'-z')_{\rm o} - (i'-z')_{\rm o,zp}][X - X_{\rm zp}] , \end{aligned} \quad (4)$$

$$\begin{aligned} z'_{\rm inst} &= z'_{\rm o} + a_z + k_z X \\ &\quad + b_z[(i'-z')_{\rm o} - (i'-z')_{\rm o,zp}] \\ &\quad + c_z[(i'-z')_{\rm o} - (i'-z')_{\rm o,zp}][X - X_{\rm zp}]. \end{aligned} \quad (5)$$

Taking the g' equation as an example, we note that $g'_{\rm inst}$ is the measured instrumental magnitude, $g'_{\rm o}$ is the extra-atmospheric magnitude, $(g'-r')_{\rm o}$ is the extra-atmospheric color, a_g is the nightly zero point, k_g is the first order extinction coefficient, b_g is the system transform coefficient, c_g is the second order (color) extinction coefficient, and X is the airmass of the observation. The zeropoint constants, $X_{\rm zp}$ and $(g'-r')_{\rm o,zp}$ were defined, respectively, to be the average standard star observation airmass $< X > = 1.3$ and the "cosmic color," as listed in Table 3 of Smith et al. (2002). Note that the above equations differ from their analogs in Smith et al. (2002) by the inclusion of zeropoint colors in the system transform ("b") terms. (Note also that there are some differences in the calibration methodology used in the current paper as opposed to that now used in standard photometric calibrations of the SDSS imaging data. In particular, standard SDSS calibrations now use different values for the zeropoint colors; further, standard SDSS calibrations now index the i' filter to $(r'-i')$ and not to $(i'-z')$; for more details see Tucker et al. 2006.)

Third, in Smith et al. (2002), since we used one telescope (the USNO 1-m) for all the observations in setting up the original $u'g'r'i'z'$ standard star network, we set all values of the system transform ("b") coefficients identically to zero. Here, we are using a different telescope, so we solve for these "b" terms.

Fourth, instead of using the first-order inverse photometric equations to convert from instrumental magnitudes to calibrated magnitudes in `kali` (eqs. 9 – 13 of Smith et al. 2002), the current version of `MTPIPE` does this conversion by solving the above equations iteratively.

The night characterization data from `MTPIPE` for each of the photometric nights included in this project are given in Table 4. (A night, or portion thereof, was declared to be photometric if the rms scatter in the residuals from the `excal` fits to photometric equations was not greater than 0.040 mag for u' and z' and no greater than 0.025 mag for

g', r' and i'.) These data include the MJD of observation (column 1), filter (column 2), zero points (column 3), system transformation terms (column 4), and first-order extinction terms (columns 5 through 7). Note that the zero points and system transformation terms are solved on a night-by-night basis; since it is not uncommon for the first-order extinctions to vary during a night, we typically solve for them in 3-hour-long blocks of time. Finally, columns 8 and 9 give the rms errors for, and numbers of, the standard stars observed that night which were used in the photometric solutions. The weighted mean averages are listed by filter at the bottom of the table as an aid to observers looking for mean site values. In a footnote, we also list the second order extinction terms derived in Smith et al. (2002).

EDITOR: PLACE TABLE 4 HERE.

Figure 5 shows the photometric zeropoint versus MJD for each filter. We see the slight degradation of telescope throughput with time, a result of the mirror not being re-aluminized over the course of this program. The mirror cleaning after the second observing run is evident as a dip in the values of the photometric zeropoint in all five filters near MJD 52085. Figure 5 of Smith et al. (2002) shows similar trends for the USNO-1.0m telescope, but the effect of the re-aluminization of that telescope is clearly seen. Figure 6 shows the first order extinction coefficients for each reduction block by MJD and Figure 7 shows the instrumental color terms (determined nightly) vs. MJD over the course of this program. Note that there are no obvious strong seasonal trends in either the first-order extinction coefficients or the instrumental color terms at CTIO for this filter set. (There might be a low-amplitude seasonal trend in the first-order extinctions.) As seen, all these nights used for calibrating the southern standards were well behaved.

For quality assurance, the residuals from all the `excal` solutions over the course of the survey program were examined for trends as a function of many different variables (Figs 8

– 15). In general, we found no apparent trends in the residuals as a function of MJD (Fig. 8)[17], airmass (Fig. 9), magnitude (Fig. 10), color (Fig. 11), color × airmass (Fig. 12), right ascension (Fig. 13), declination (Fig. 14), and hour angle (Fig. 15).

We note, however, that there does appear to be a small trend in the u' residuals vs. color and vs. color×airmass. In both cases, the amplitude of the effect seems to be about 0.02 – 0.03 mag over the full range of $u' - g'$ colors (Figs. 11 and 12). We suspect this trend indicates that the instrumental response color term coefficient (the "b" term coefficient) is not single-valued for the CTIO u' filter, but may require different values for blue and red stars. We note also that this effect translates into the plot of u' residuals vs. right ascension, since bluer (redder) Smith et al. (2002) standards were observed preferentially at various values of right ascension (Figs. 16 and 17). Resolving this issue is one of the goals for version 2 of the Southern $u'g'r'i'z'$ standard star network (Smith et al., in preparation).

EDITOR: PLACE FIGURE 5 HERE.

EDITOR: PLACE FIGURE 6 HERE.

EDITOR: PLACE FIGURE 7 HERE.

EDITOR: PLACE FIGURE 8 HERE.

---

[17]Since we did night-by-night `excal` solutions rather than a global solution, it is not surprising that there is no trend in the residuals vs. MJD.

EDITOR: PLACE FIGURE 9 HERE.

EDITOR: PLACE FIGURE 10 HERE.

EDITOR: PLACE FIGURE 11 HERE.

EDITOR: PLACE FIGURE 12 HERE.

EDITOR: PLACE FIGURE 13 HERE.

EDITOR: PLACE FIGURE 14 HERE.

EDITOR: PLACE FIGURE 15 HERE.

EDITOR: PLACE FIGURE 16 HERE.

EDITOR: PLACE FIGURE 17 HERE.

3.2. Post-MTPIPE Processing

At this point in the reduction process using MTPIPE, we had several calibrated object lists for each field, one list for each of the photometric exposures in each field. To ensure a clean sample for each field, lists with photometric offsets that deviated from a field's median averaged list by more than 0.10 mag in u' or more than 0.05 mag in $g'r'i'z'$ were discarded from further analysis. We then combined the remaining lists for each field by taking the (unweighted) mean magnitude of each object in each filter. To avoid problems associated with signal-to-noise mismatches between the long and the short exposures, we only included in the mean magnitudes those measurements having photon noise errors of ≤ 0.05 mag. We excluded saturated measurements from the mean magnitude calculations. The resulting list of candidate standards contained approximately 92,000 candidate objects.

We culled this list using the following criteria:

- The mean magnitude in r' must have been derived from at least five good individual measurements, AND at least three good measurements in g' and i'. This logical AND statement is an effective cosmic ray filter.
- The standard deviation of the individual measurements in r' must be less than 0.10 mag (to avoid variables).
- The error in the mean magnitude in r' (standard deviation of the mean) must be less than 0.03 mag (to be useful as a standard star). This effectively creates a faint limit for each field, based on exposure time.

After culling the MTPIPE output using the above criteria, we were left with about 17,600 candidates. We used the resulting list to perform a coordinate match with the 2MASS data base to do a color-based star-galaxy separation and to obtain 2MASS designations for each of our sources. An additional check versus the NED helped to identify any remaining galaxies. In some survey fields (i.e. DLS, CDFS) we referred to those catalogs for star-galaxy information. The final list presented here contains 16,003 secondary standard stars.

3.3. The Red Leak Correction

Due to two small red leaks in the USNO 1.0m telescope's u' filter — one at 8120Å and another, larger leak beyond 10,000Å — we were obliged in Smith et al. (2002) to apply a red leak correction to the u'-band magnitudes for the original set of northern+equatorial $u'g'r'i'z'$ standards (see § 4.3 of Smith et al. 2002). In the USNO 1.0m telescope's data, this red leak correction only became significant (>0.01 mag) for stars redder than $u' - i' = 5$, or for about 10% of the Smith et al. (2002) sample (see Fig. 15 of Smith et al. 2002);

Filter transmission curves for a similar set of $u'g'r'i'z'$ filters (resident at University of Wyoming) from the same manufacturer (Custom Scientific) indicate that there are likely comparable red leaks in the CTIO 4-in u' filter used for the current program. Therefore, we expect non-negligible (> 0.01 mag) red leak corrections for u'-band measurements of stars in our current sample redder than about $u' - i' = 5$. Since the calculation of red leak corrections requires highly accurate and precise measurements of very small features at non-standard wavelengths in the filter transmission curves, and since these rather specialized measurements are not currently available for the CTIO 4-in u' filter, we have decided to defer calculating and applying these corrections to a future version of this southern $u'g'r'i'z'$ standard star catalog. We therefore recommend that users of the current catalog do not include very red stars ($u' - i' > 5$) when calibrating u'-band data. As an added caveat, these stars have been marked with an asterisk in our current catalog (see § 4). Out of 16,003 standard stars in our current catalog, only 187 — or about 1% — are red enough to be so marked.

4. The Southern Standard Star Network

4.1. The Data Tables and Graphical Summary Pages

Here, we present the calibrated $u'g'r'i'z'$ magnitude and data for Southern $u'g'r'i'z'$ standard stars. The data tables are arranged by a field-by-field basis and are available from our website at `http://www-star.fnal.gov`. Here, we give as an example the table for field DLS_0520-49 (Table 5). The table entries are arranged in order of increasing right ascension, and the columns are as follows: *(column 1)* the star name, using the IAU-registered naming convention ugriz JHHMMSS.s±DDMMSS; *(columns 2–3)* the star's right ascension and declination (J2000); *(columns 4–6)* the star's u' magnitude, the 1σ rms error in its u' magnitude, and the number of individual measurements that were used to determine its u' magnitude, respectively; *(columns 7–9)* likewise for g'; *(columns 10–12)* likewise for r'; *(columns 13–15)* likewise for i'; *(columns 16–18)* likewise for z'; *(columns 19–20)* the distance $D_{\rm NN}$ from the star to its nearest detected neighbor in units of arcseconds and in units of aperture radii (arcsec/7.43″; see § 3.1), respectively; and *(column 21)* where an asterisk indicates that the star has a $u' - i'$ color redder than 5 and thus might have a significant (>0.01 mag) uncorrected red leak contamination in its u' magnitude. Those performing photometry but not using the aperture size we used in extracting the standard stars should use only those standards with $D_{\rm NN} \geq 14.86''$ ($\geq$ 2 aperture radii). Those concerned with accurate u'-band photometry should exclude stars with $u' - i' > 5$ from their u'-band photometric solutions.

Figure 18 shows an example of the graphical summary page built for each field. As with the table, this example is for the DLS_0520-49 field. The page includes an r'-band image of the field, an r'-magnitude histogram in half-magnitude steps, and a $(g' - r')$ histogram an aid to the observers. Also included on this page are plots showing the rms errors (the standard deviation of the mean) in the calibrated magnitudes versus the calibrated magnitude for the standards in each of the five filters and a plot of the rms errors for the calibrated magnitudes versus the color for the standards in each of the filters.

EDITOR: PLACE FIGURE 18 HERE.

4.2. The Global Characteristics

The global distributions of the final set of standards by r'-band magnitude and $(g' - r')$ color are shown in Figures 19a and 19b. The magnitude distribution plot shows the effect of varying exposure times in the different fields.

EDITOR: PLACE FIGURE 19a HERE.

EDITOR: PLACE FIGURE 19b HERE.

The color-color space distributions of the final set of stars are shown in Figure 20a $(u' - g')$ vs. $(g' - r')$, Figure 20b $(g' - r')$ vs. $(r' - i')$, and Figure 20c $(r' - i')$ vs. $(i' - z')$. The break in the linear color transforms at about spectral type M0 is clearly seen in Figure 20b and is also evident in Figure 20c. Separation of the metal-poor stars from the main sequence dwarfs is seen in Figure 20a. The clump of stars in the blue-blue corner of all three of these plots are the warm-hot white dwarfs.

EDITOR: PLACE FIGURE 20a HERE.

EDITOR: PLACE FIGURE 20b HERE.

EDITOR: PLACE FIGURE 20c HERE.

4.3. Transformation Relations from $UBVRI$

Approximate relations for transforming magnitudes and colors from the Johnson–Morgan–Cousins $UBVR_cI_c$ to the SDSS $u'g'r'i'z'$ filter system were given in the system defining paper (Fukugita et al. 1996) and updated in Smith et al. (2002). Since the basis of this extension is the original network, there are no changes to these transformation equations due to this work. Expanded transformation equations are given in Karaali et al. (2005) and Rodgers et al. (2006). Karaali et al. (2005) produced new transformation equations for the UBV to $u'g'r'$ filters using color-color relations similar to Smith et al. (2002), but adding a second color dependence for each equation, to wit, the $(u' - g')$ and $(g' - r')$ colors are related to both $(U - B)$ and $(B - V)$ colors. This is due to the non-linear dependence of g' on B and V. Rodgers et al. (2006) extend the Karaali et al. (2005) work by transforming $UBVR_cI_c$ to $u'g'r'i'z'$, but note that they also identify a luminosity class dependence. They present the transformation equations for luminosity class V stars only. These equations will be useful in determining reddening vectors, distances, and ages for stellar systems with main-sequence stars. Rodgers et al. (2006), among others, are currently expanding this work for other luminosity classes and also intend to include metallicity terms. Though the original SDSS standard stars do not go redder than about M0 Davenport et al. (2007) gives a good overview of transformation work on the red end and compute color transformations for cool stars between the $ugriz$, $UBVRI$, and 2MASS JHK' systems.

5. Future Work

Development of standard star networks, especially those intended to be of significant use to the astronomical community, is a never-ending process. Even though the basic system has been developed, improvements can always be made. The $u'g'r'i'z'$ system is no exception. The standard stars released in this paper establish the basic southern network. As mentioned before, these are fainter than the northern network, in part to accommodate larger telescopes. The large number of stars is built with large surveys (and telescopes) in mind. There will be more stars added in the future. These will primarily be in fields that contained existing standards and these were not completely reduced as unknowns. We are going back to extract these additional stars which will be uploaded to the website.

With the southern extention available, we also turn our attention back to the northern hemisphere network. A project which we have begun to work on is an enhancement of the northern system to develop fainter standards, comparable to those now available in the southern hemisphere. These data come from two sources. First, we have re-reduced the original northern observations to extract all stars from the images. During the original reductions we only dealt with the pre-selected stars to meet the SDSS calibration needs. Second, we have begun a new series of observations using the USNO 1m telescope and detector used to develop the original standard system (see Smith et al. 2002). Several of these fainter standards will be in the existing northern fields, and will be two to four magnitudes fainter. Further, to support the galactic study component of the SDSS-II, we are not restricting the color range of the new standards. This will primarily be manifested by redder stars. Fields of special interest, such as the DLS northern fields, will also be targetted during the new observations.

The availability of high precision photometric measurements and high resolution spectroscopy has made the viability of a photometric-metallicity system possible. A concern with this is are the $u'g'r'i'z'$ filters sensitive enough for this work. A pilot project to test this is underway as part of the northern enhancement work. Part of this effort also targets stellar clusters of known metallicity and ages. These data may be useful for future isochrone refinements.

We dedicate this work to the memory of Bev Oke, one of the premier optical instrumentalists in the United States during the 1960s through the 1980s. Indeed, his work on CCDs and spectrographs laid much of the groundwork for the development of the SDSS instrumentation. Bev played an advisory role to the SDSS early in the project, sitting on several review panels as the project was getting started. For us, Bev did much of the early work on setting up photometric and spectrophotometric standards, and invented the AB magnitude system which is employed by the SDSS. This pioneering work deeply influenced the SDSS photometric calibration. To this end, Bev also served as the referee on the first $u'g'r'i'z'$ standard star paper and his comments made that paper much more robust. It was a pleasure to benefit from his guidance in that initial effort and he will be sorely missed in future endeavors.

The authors also acknowledge the many useful discussions of this project, and standard stars in general, with Arlo Landolt, Brian Skiff, Arne Henden and Nick Suntzeff. Also, we thank the CTIO staff, especially Edgardo Cosgrove, Arturo Gomez, Nick Suntzeff and Stefanie Wachter, for their support.

This material is based upon work supported by the National Science Foundation under Grant No. AST 0098401 and made use of the National Optical Astronomy Observatories Survey Program. JAS and JLS received partial support from the Los Alamos National Lab grant No. LDRD-20030486DR. DLT was supported by the US Department of Energy under contract No. DE-AC02-76CH03000.

The Guide Star Catalogue-II is a joint project of the Space Telescope Science Institute and the Osservatorio Astronomico di Torino. Space Telescope Science Institute is operated by the Association of Universities for Research in Astronomy, for the National Aeronautics and Space Administration under contract NAS5-26555. The participation of the Osservatorio Astronomico di Torino is supported by the Italian Council for Research in Astronomy. Additional support is provided by European Southern Observatory, Space Telescope European Coordinating Facility, the International GEMINI project and the European Space Agency Astrophysics Division.

The Guide Star Catalog-I was produced at the Space Telescope Science Institute under U.S. Government grant. These data are based on photographic data obtained using the Oschin Schmidt Telescope on Palomar Mountain and the UK Schmidt Telescope.

The EIS data are based on observations carried out using the MPG/ESO 2.2m Telescope and the ESO New Technology Telescope (NTT) at the La Silla observatory under Program-ID No. 164.0-0561.

This research has made use of the SIMBAD database, operated at CDS; the VizieR catalog access tool, CDS; and the Aladin, developed by CDS, Strasbourg, France.

This research has made use of the NASA/IPAC Extragalactic Database (NED) which is operated by the Jet Propulsion Laboratory, California Institute of Technology, under contract with the National Aeronautics and Space Administration.

This research has made use of data obtained from or software provided by the US National Virtual Observatory, which is sponsored by the National Science Foundation.

This publication makes use of data products from the Two Micron All Sky Survey, which is a joint project of the University of Massachusetts and the Infrared Processing and Analysis Center/California Institute of Technology, funded by the National Aeronautics and Space Administration and the National Science Foundation.

REFERENCES

Alvarado, F., Wenderoth, E., Alcaíno, G., & Liller, W. 1995, AJ, 110, 646

Bennett et al. 1963, Journal of the Optical Society of America, 53, 1083

Bok, B. J., & Bok, P. F. 1969, AJ, 74, 1125

Davenport, J.R.A., West, A.A., Matthiesen, C.K., Schmieding, M., & Kobelski, A. 2007, PASP, in press

Fukugita, M., Ichikawa, T., Gunn, J. E., Doi, M., Shimasaku, K., & Schneider, D. P. 1996, AJ, 111, 1748

Graham, J. A. 1981, PASP, 93, 29

Graham, J. A. 1982, PASP, 94, 244

Gunn, J. E., Carr, M., Rockosi, C., Sekiguchi, M., et al. 1998, AJ, 116, 3040

Hogg, D. W., Finkbeiner, D. P., Schlegel, D. J., & Gunn, J. E. 2001, AJ, 122, 2129

Gunn, J. E., Siegmund, W. A., Mannery, E. J., et al. 2006, AJ, 131, 2332

Ivezić, Ž., Lupton, R. H., Schlegel, D., et al. 2004, Astr. Nachr., 325, 583

Ivezić, Ž., Smith, J. A., Miknaitis, G., et al. 2007, in *The Future of Photometric, Spectrophotometric, and Polarimetric Standardization*, ed. C. Sterken, in press

Karaali, S., Bilir, S., Tunçel, S. 2005, PASA, 22, 24

Kneale, R. 1994, "Functional Specification for the Gemini Coating Plants," SPE-TE-G0043

Landolt, A. U. 1973, AJ, 78, 959

Landolt, A. U. 1983a, AJ, 88, 439

Landolt, A. U. 1983b, AJ, 88, 853

Landolt, A. U. 1992, AJ, 104, 372

Lupton, R. H., Gunn, J. E., & Szalay, A. S. 1999, AJ, 118, 1406

Oke, J. B., & Gunn, J.E. 1983, ApJ, 266, 713.

Rodgers, C. T., Canterna, R., Smith, J. A., Pierce, M. J., & Tucker, D. L. 2006, AJ, 132, 989

Smith, J. A., Tucker, D. L., Kent, S. et al. 2002, AJ, 123, 2121.

Smith, J. A., Tucker, D. L., Allam, S.S., & Rodgers, C. T. 2003, AJ, 126, 2037.

Smith, J. A., Tucker, D. L., Allam, S.S., et al. 2007, in *The Future of Photometric, Spectrophotometric, and Polarimetric Standardization*, ed. C. Sterken, in press

Stoughton, C., Lupton, R. H., Bernardi, M. et al. 2002, AJ, 123, 485.

Tucker, D. L., Kent, S., Richmond, M. W. et al. 2006, Astr. Nachr., 327, 821

York, D. G., Adelman, J., Anderson, J. E. et al. 2000, AJ, 120, 1579

This manuscript was prepared with the AAS LaTeX macros v5.0.

Table 1. Observing Runs for the CTIO 0.9-m Telescope

YYMM	UT Dates	mjd	Nights	Clear[a]	# Obs.[b]
0009	09/19–09/25	51806–51812	7	5	96
0103	03/27	51995	1	0	0
	03/29–04/02	51997–52001	5	3	80
0106	06/23–06/29	52083–52089	7	4	111
0109	09/19–09/25	52171–52177	7	2	77
0202	02/01–02/08	52306–52313	8	7	171
0205	05/25–05/31	52419–52425	7	1	9
0210	10/05–10/11	52552–52558	7	7	257
0302	02/10–02/16	52680–52686	7	7	132
0307	07/18–07/24	52838–52844	7	1	43
0309	09/15–09/21	52898–52904	7	0	0
0401	01/27–02/02	53031–53037	7	7	218
0405	05/07–05/13	53132–53138	7	5	163
$\sum$			84	49	1357

[a]Here, a "clear" night is as judged at the telescope by the observer and with clear conditions persisting at least 2 hours in duration.

[b]Number of existing standards observed, based on the r'-band data.

Table 2. CCD Parameters

Side	Gain (epadu)	Read Noise (e^-)
upper Left	3.1	4.7
lower Left	3.0	5.4
upper Right	3.0	4.6
lower Right	3.0	5.1

Table 3. Centers for each Observed Field

Field Name	RA	Dec.	Exposure Time [sec]					Notes
	J2000		r'	g'	u'	i'	z'	
Original Standard Stars								
G158-100	00:33:54	-12:07:57	40	80	480	40	80	
SA_92-A	00:55:17	+00:39:34	9	15	90	14	22	
SA_92-D	00:57:04	+00:40:30	14	20	160	14	33	
SA_93-A	01:54:51	+00:44:32	9	15	90	14	22	
SA_93-B	01:55:26	+00:56:54	6	10	120	6	9	
SA_94-A	02:57:33	+00:17:36	7	10	70	7	12	
SA_95-C	03:53:17	+00:16:45	30	40	360	30	40	
SA_95-D	03:55:00	+00:05:23	15	20	150	15	20	
SA_95-F	03:55:56	+00:10:12	5	6	60	5	6	
BD-21o0910	04:33:12	-21:07:00	5	5	30	5	7	
SA_96-A	04:51:30	-00:12:10	10	14	90	14	25	
SA_96-B	04:52:35	+00:22:50	9	15	90	14	22	
SA_96-C	04:53:09	-00:10:45	9	15	90	14	22	
SA_97-A	05:56:48	+00:01:34	9	16	100	10	25	
SA_97-C	05:57:31	+00:17:00	6	8	150	6	7	
SA_98-B	06:51:59	-00:22:36	5	5	25	5	6	
Ru-149	07:24:14	-00:31:41	13	15	150	15	33	
SA_99-A	07:56:00	-00:18:47	5	5	20	5	8	
SA_100-B	08:53:46	-00:34:14	10	20	200	10	25	
BD-12o2918	09:31:19	-13:29:18	5	8	120	5	5	
SA_101-A	09:54:52	-00:23:38	10	14	120	10	15	
G162-66	10:33:42	-11:41:39	15	15	60	25	60	
PG_1047+003	10:50:05	-00:01:11	25	30	200	35	45	
G163-50/51	11:07:38	-05:11:37	20	30	200	20	30	
SA_103-A	11:56:40	-00:27:22	8	8	90	8	10	
SA_104-A	12:41:47	-00:28:00	16	20	200	20	30	
PG_1323-086	13:25:49	-08:50:22	20	25	150	30	40	
SA_105-A	13:40:04	-00:02:19	7	12	60	8	12	
BD+26o2606	14:49:02	+25:42:27	5	7	50	5	9	
LHS_0394	15:19:31	-07:43:36	5	10	150	5	5	

Table 3—Continued

Field Name	RA	Dec.	Exposure Time [sec]					Notes
	J2000		r'	g'	u'	i'	z'	
PG_1528+062	15:30:48	+06:01:05	15	15	120	15	20	
SA_107-B	15:38:56	-00:37:13	15	15	90	15	25	
SA_108-B	16:37:47	-00:33:27	6	8	60	10	18	
SA_109-A	17:44:09	-00:23:08	10	12	100	10	15	
SA_109-B	17:45:31	-00:24:05	5	5	60	5	5	
Hiltner_733	18:17:12	-11:44:00	9	15	150	9	12	
SA_110-B	18:41:41	+00:11:28	5	5	60	5	9	
SA_110-D	18:43:12	+00:30:46	9	12	180	8	11	
SA_110-E	18:43:43	+00:20:59	8	10	120	8	10	
SA_111-B	19:37:39	+00:28:16	7	9	120	5	6	
SA_112-AB	20:42:32	+00:12:31	8	10	90	8	10	
SA_113-C	21:41:42	+00:20:43	15	20	150	12	15	
G93-48	21:52:12	+02:22:45	15	20	300	20	40	
BD+17o4708	22:11:31	+18:05:34	5	5	40	5	7	
BD-11o5781	22:13:10	-11:10:39	5	5	50	5	6	
SA_114-A	22:44:51	+00:48:52	10	20	120	10	20	
SA_114-C	22:41:41	+01:11:14	10	20	150	10	22	
PG_2336+004	23:38:41	+00:42:42	16	20	150	16	30	
SA_115-A	23:42:18	+01:07:27	10	15	120	15	30	
New Fields								
000000-295830	00:00:00	-29:58:30	15	15	135	15	23	
			90	90	810	90	140	
000000-600000	00:00:00	-60:00:00	15	15	135	15	23	
			90	90	810	90	140	
SA_140-A	00:03:38	-28:39:40	15	20	180	15	20	Landolt (1983b)
JL_163	00:10:50	-50:15:00	40	40	360	40	60	Landolt - private communication
TPhe-B	00:30:38	-46:27:55	25	30	480	30	60	Landolt - private communication
						15	30	extra exposures for the red stars
NGC_300-A	00:54:42	-37:55:48	20	35	300	30	40	Graham (1981)
			120	210	1800	180	240	

Table 3—Continued

Field Name	RA	Dec.	Exposure Time [sec]					Notes
	J2000		r'	g'	u'	i'	z'	
NGC_458-A	01:13:37	-71:33:00	20	35	480	30	40	Alvarado et al. (1995)
NGC_458-B	01:15:15	-71:33:00	20	35	480	30	40	merged with NGC_458-A to form NGC_458-AB in final data tables
E1-A	01:24:50	-44:38:40	20	35	480	30	40	Graham (1982)
E1-B	01:24:08	-44:23:23	5	5	40	5	7	
			30	30	480	40	60	
020000-300600	02:00:00	-30:06:00	15	15	135	15	23	
			90	90	810	90	140	
020020-600000	02:00:20	-60:00:00	15	15	135	15	23	
			90	90	810	90	140	
CDFS	03:32:28	-27:48:30	20	25	150	20	30	
			180	180	1440	180	240	
040004-295900	04:00:04	-29:59:00	15	15	135	15	23	
			90	90	810	90	140	
040020-600200	04:00:20	-60:02:00	15	15	135	15	23	
			90	90	810	90	140	
E2-A	04:03:00	-44:46:45	30	50	480	40	60	Graham (1982)
NGC_1841	04:45:00	-84:00:00	60	100	900	80	120	Alvarado et al. (1995)
DLS_0520-49	05:20:00	-49:00:00	20	25	150	20	30	Tyson - private communication
			120	150	900	120	180	
060000-300000	06:00:00	-30:00:00	15	15	135	15	23	
			90	90	810	90	140	
055950-595600	05:59:50	-59:56:00	15	15	135	15	23	
			90	90	810	90	140	
E3-A	06:42:54	-45:10:06	7	8	60	9	15	Graham (1982)
			30	50	480	40	60	
080000-300000	08:00:00	-30:00:00	15	15	135	15	23	
			90	90	810	90	140	
075944-595500	07:59:44	-59:55:00	20	20	150	20	30	
			120	120	900	120	180	
WD_0830-535	08:31:51	-53:40:44	45	60	600	60	75	Landolt - private communication
E4-A	09:23:44	-45:26:02	5	5	40	5	7	Graham (1982)

Table 3—Continued

Field Name	RA	Dec.	Exposure Time [sec]					Notes
	J2000		r'	g'	u'	i'	z'	
			45	60	480	60	75	
PG_0942-029	09:45:12	-03:06:57	40	60	480	40	60	Landolt - private communication
100000-300000	10:00:00	-30:00:00	15	15	135	15	23	
			90	90	810	90	140	
100000-600000	10:00:00	-60:00:00	15	15	135	15	23	
			90	90	810	90	140	
GD108	10:00:47	-07:33:31	20	30	420	30	50	Landolt - private communication
DLS_1052-05	10:52:00	-05:00:00	20	25	150	20	30	Tyson - private communication
			120	150	900	120	180	
WD_1056-384	10:58:17	-38:44:35	30	40	420	40	60	Landolt - private communication
IC_2944-A	11:35:49	-63:12:10	20	35	480	30	40	Bok & Bok (1969)
IC_2944-B	11:33:43	-63:02:09	20	35	480	30	40	merged with IC_2944-A to form IC_2944-AB in final data tables
120000-295355	12:00:00	-29:53:55	15	15	135	15	23	
			90	90	810	90	140	
120000-600000	12:00:00	-60:00:00	15	15	135	15	23	
			90	90	810	90	140	
E5-A	12:04:11	-45:29:03	5	8	150	5	8	Graham (1982)
E5-B	12:05:16	-45:34:07	60	70	600	75	90	
LSE_44	13:52:49	-48:09:09	15	20	360	25	30	Landolt - private communication
DLS_1359-11	13:59:20	-11:03:00	20	25	150	20	30	Tyson - private communication
			120	150	900	120	180	
140000-300000	14:00:00	-30:00:00	15	15	135	15	23	
			90	90	810	90	140	
140000-600000	14:00:00	-60:00:00	15	15	135	15	23	
			90	90	810	90	140	
E6-A	14:45:33	-45:20:34	5	5	75	7	12	Graham (1982)
E6-B	14:46:25	-45:29:04	30	30	480	30	45	
160100-300000	16:01:00	-30:00:00	15	15	135	15	23	
160100-600000	16:01:00	-60:00:00	90	90	810	90	140	
SA_132-A	16:18:41	-15:09:23	5	15	240	5	5	Landolt (1983b)
PG_1633+099	16:35:32	+09:47:50	30	40	480	40	60	Landolt - private communication

Table 3—Continued

Field Name	RA	Dec.	Exposure Time [sec]					Notes
	J2000		r'	g'	u'	i'	z'	
LSE_259	16:53:54	-56:02:00	5	7	75	5	9	Landolt - private communication
			30	30	480	40	60	Landolt - private communication
E7-A	17:27:22	-45:00:33	30	50	480	45	60	Really crowded, not used.
180000-300000	18:00:00	-30:00:00						Really crowded, not used.
180000-600000	18:00:00	-60:00:00	15	15	135	15	23	
			90	90	810	90	140	
190000-295600	19:00:00	-29:56:00	15	15	135	15	23	
			90	90	810	90	140	
200000-300000	20:00:00	-30:00:00	15	15	135	15	23	
			90	90	810	90	140	
195940-595000	19:59:40	-59:50:00	15	15	135	15	23	
			90	90	810	90	140	
E8-A	20:07:22	-44:42:01	30	50	480	40	60	Graham (1982)
E8-B	20:04:23	-45:00:22	5	5	40	5	7	
MCT_2019	20:22:48	-43:29:32	30	40	480	40	70	Landolt - private communication
JL_82	21:36:06	-72:49:00	20	30	300	25	30	Landolt - private communication
220100-300000	22:01:00	-30:00:00	15	15	135	15	23	
			90	90	810	90	140	
220000-595900	22:00:00	-59:59:00	15	15	135	15	23	
			90	90	810	90	140	
E9-A	22:45:37	-44:27:47	45	60	480	60	75	Graham (1982)
E9-B	22:44:51	-44:37:42	7	8	60	9	15	

Table 4. Night Characterization Coefficients & Averages*

MJD	Filter	Zeropoint (a)	Instr. Color (b)	1st-Order Ext. (k) block 0	block 1	block 2	Std. rms (mag)	# Std. stars
(1)	(2)	(3)	(4)	(5)	(6)	(7)	(8)	(9)
				07:30-09:31UT				
51808	u'	-21.074±0.010	-0.010±0.006	0.517±0.006	···	···	0.005	4
51808	g'	-22.727±0.005	0.007±0.005	0.192±0.003	···	···	0.002	6
51808	r'	-22.624±0.020	-0.104±0.039	0.094±0.009	···	···	0.008	6
51808	i'	-22.141±0.032	-0.071±0.077	0.058±0.012	···	···	0.011	6
51808	z'	-21.236±0.022	0.016±0.052	0.049±0.008	···	···	0.008	6
				01:17-04:17UT	04:17-09:20UT			
51809	u'	-21.032±0.019	0.011±0.015	0.462±0.012	0.470±0.014	···	0.021	15
51809	g'	-22.657±0.019	0.072±0.017	0.169±0.011	0.158±0.010	···	0.013	15
51809	r'	-22.597±0.015	-0.029±0.037	0.090±0.008	0.085±0.008	···	0.013	16
51809	i'	-22.107±0.016	-0.031±0.036	0.053±0.006	0.050±0.008	···	0.012	15
51809	z'	-21.168±0.015	0.109±0.041	0.048±0.006	0.053±0.006	···	0.010	15
				23:49-02:49UT	02:49-06:24UT			
51810	u'	-20.989±0.025	-0.018±0.012	0.443±0.017	0.445±0.018	···	0.023	18
51810	g'	-22.677±0.008	0.049±0.005	0.164±0.005	0.169±0.005	···	0.007	21
51810	r'	-22.595±0.010	-0.046±0.012	0.085±0.005	0.086±0.006	···	0.009	20
51810	i'	-22.115±0.015	-0.048±0.024	0.062±0.006	0.064±0.008	···	0.009	20
51810	z'	-21.188±0.017	-0.016±0.033	0.061±0.007	0.068±0.009	···	0.011	18
				03:57-09:09UT				
51811	u'	-20.988±0.028	-0.003±0.012	0.514±0.021	···	···	0.017	20
51811	g'	-22.674±0.010	0.062±0.007	0.224±0.009	···	···	0.012	45
51811	r'	-22.610±0.012	-0.030±0.015	0.131±0.010	···	···	0.010	24
51811	i'	-22.107±0.011	0.009±0.022	0.073±0.009	···	···	0.008	23
51811	z'	-21.204±0.012	0.058±0.025	0.056±0.010	···	···	0.009	25
				00:05-03:05UT	03:05-06:05UT	06:05-09:10UT		
51812	u'	-21.031±0.019	-0.041±0.009	0.504±0.015	0.519±0.013	0.497±0.013	0.019	27
51812	g'	-22.682±0.008	0.044±0.006	0.215±0.006	0.208±0.006	0.187±0.006	0.010	34
51812	r'	-22.600±0.008	-0.030±0.012	0.123±0.005	0.120±0.006	0.106±0.006	0.010	30
51812	i'	-22.116±0.012	-0.036±0.025	0.067±0.007	0.068±0.007	0.051±0.007	0.013	34
51812	z'	-21.221±0.013	0.011±0.028	0.053±0.007	0.067±0.007	0.048±0.008	0.013	29
				01:08-04:08UT	04:08-09:47UT			
51997	u'	-20.974±0.033	-0.043±0.015	0.547±0.019	0.540±0.020	···	0.025	22
51997	g'	-22.549±0.017	0.036±0.010	0.194±0.008	0.195±0.008	···	0.010	23
51997	r'	-22.504±0.011	-0.049±0.013	0.095±0.006	0.098±0.006	···	0.007	22
51997	i'	-21.970±0.015	0.015±0.027	0.045±0.008	0.046±0.008	···	0.011	24
51997	z'	-21.194±0.026	-0.104±0.046	0.073±0.013	0.084±0.013	···	0.019	24
				00:23-03:23UT	03:23-06:23UT	06:23-09:55UT		

Table 4—Continued

MJD	Filter	Zeropoint (a)	Instr. Color (b)		1st-Order Ext. (k)		Std. rms	# Std.
				block 0	block 1	block 2	(mag)	stars
(1)	(2)	(3)	(4)	(5)	(6)	(7)	(8)	(9)
51998	u'	-20.882±0.020	-0.040±0.008	0.493±0.014	0.502±0.013	0.490±0.014	0.020	31
51998	g'	-22.522±0.012	0.037±0.007	0.178±0.008	0.186±0.008	0.191±0.008	0.011	33
51998	r'	-22.482±0.010	-0.048±0.011	0.080±0.007	0.092±0.006	0.096±0.006	0.009	33
51998	i'	-22.002±0.010	-0.043±0.017	0.050±0.006	0.058±0.006	0.065±0.006	0.009	33
51998	z'	-21.104±0.017	0.022±0.028	0.050±0.010	0.059±0.010	0.063±0.010	0.015	32
				00:00-03:00UT	03:00-06:00UT	06:00-10:05UT		
52000	u'	-20.928±0.032	-0.057±0.009	0.509±0.021	0.491±0.022	0.487±0.022	0.029	25
52000	g'	-22.527±0.008	0.032±0.004	0.172±0.005	0.167±0.006	0.167±0.006	0.006	22
52000	r'	-22.509±0.026	-0.078±0.020	0.090±0.016	0.080±0.018	0.084±0.018	0.022	25
52000	i'	-22.008±0.014	-0.048±0.016	0.052±0.008	0.049±0.009	0.051±0.009	0.011	25
52000	z'	-21.118±0.021	0.012±0.024	0.063±0.012	0.055±0.013	0.050±0.013	0.017	25
				00:25-03:25UT	03:25-06:25UT	06:25-10:34UT		
52084	u'	-21.059±0.021	-0.032±0.006	0.482±0.014	0.465±0.013	0.479±0.014	0.020	32
52084	g'	-22.604±0.014	0.041±0.006	0.157±0.009	0.152±0.008	0.150±0.009	0.012	34
52084	r'	-22.617±0.010	-0.039±0.008	0.101±0.007	0.086±0.007	0.085±0.007	0.010	35
52084	i'	-22.143±0.017	0.009±0.021	0.091±0.011	0.062±0.011	0.065±0.012	0.016	35
52084	z'	-21.280±0.016	0.039±0.020	0.085±0.011	0.057±0.010	0.060±0.011	0.015	35
				23:12-02:12UT	02:12-05:12UT	05:12-10:27UT		
52085	u'	-21.087±0.023	-0.039±0.008	0.494±0.015	0.466±0.019	0.492±0.016	0.016	23
52085	g'	-22.654±0.016	0.028±0.009	0.177±0.010	0.175±0.014	0.173±0.011	0.011	23
52085	r'	-22.638±0.014	-0.050±0.016	0.096±0.009	0.092±0.013	0.091±0.010	0.010	23
52085	i'	-22.130±0.011	-0.040±0.017	0.049±0.007	0.046±0.009	0.046±0.008	0.007	22
52085	z'	-21.241±0.021	0.066±0.033	0.046±0.014	0.055±0.018	0.048±0.015	0.015	23
				23:12-02:12UT	02:12-05:12UT	05:12-10:30UT		
52086	u'	-21.050±0.050	-0.036±0.011	0.460±0.032	0.418±0.032	0.467±0.037	0.036	25
52086	g'	-22.627±0.015	0.036±0.005	0.156±0.009	0.155±0.009	0.154±0.010	0.010	24
52086	r'	-22.627±0.011	-0.064±0.008	0.083±0.007	0.085±0.007	0.081±0.008	0.008	25
52086	i'	-22.120±0.006	-0.041±0.006	0.042±0.004	0.042±0.004	0.038±0.004	0.004	23
52086	z'	-21.229±0.019	0.044±0.019	0.041±0.011	0.041±0.011	0.040±0.013	0.013	25
				03:22-10:30UT				
52088	u'	-21.086±0.044	-0.016±0.017	0.495±0.031	· · ·	· · ·	0.039	29
52088	g'	-22.636±0.027	0.046±0.014	0.173±0.017	· · ·	· · ·	0.022	28
52088	r'	-22.609±0.021	-0.034±0.021	0.084±0.014	· · ·	· · ·	0.017	28
52088	i'	-22.089±0.018	-0.036±0.028	0.025±0.012	· · ·	· · ·	0.015	29
52088	z'	-21.219±0.021	-0.005±0.033	0.025±0.014	· · ·	· · ·	0.017	29
				04:22-09:25UT				
52171	u'	-20.962±0.016	-0.025±0.007	0.480±0.011	· · ·	· · ·	0.015	30

Table 4—Continued

MJD	Filter	Zeropoint (a)	Instr. Color (b)	1st-Order Ext. (k)			Std. rms	# Std.
				block 0	block 1	block 2	(mag)	stars
(1)	(2)	(3)	(4)	(5)	(6)	(7)	(8)	(9)
52171	g'	-22.615±0.014	0.034±0.009	0.180±0.010	···	···	0.014	31
52171	r'	-22.588±0.011	-0.049±0.014	0.097±0.008	···	···	0.013	41
52171	i'	-22.111±0.014	-0.018±0.027	0.053±0.009	···	···	0.012	31
52171	z'	-21.223±0.019	0.066±0.037	0.040±0.013	···	···	0.017	31
				23:54-02:54UT	02:54-05:54UT	05:54-09:29UT		
52172	u'	-20.960±0.016	-0.016±0.007	0.459±0.012	0.484±0.012	0.475±0.012	0.018	35
52172	g'	-22.627±0.009	0.035±0.005	0.181±0.007	0.193±0.007	0.180±0.007	0.010	35
52172	r'	-22.587±0.008	-0.026±0.009	0.105±0.006	0.109±0.006	0.099±0.006	0.009	36
52172	i'	-22.120±0.010	-0.014±0.018	0.062±0.007	0.069±0.007	0.060±0.007	0.010	36
52172	z'	-21.241±0.013	0.010±0.024	0.036±0.009	0.052±0.010	0.041±0.009	0.014	36
				00:44-03:44UT	03:44-08:47UT			
52306	u'	-20.929±0.025	-0.030±0.009	0.495±0.016	0.492±0.017	···	0.021	19
52306	g'	-22.559±0.020	0.024±0.012	0.186±0.011	0.181±0.012	···	0.015	19
52306	r'	-22.536±0.011	-0.089±0.014	0.103±0.006	0.103±0.007	···	0.009	21
52306	i'	-22.035±0.016	-0.038±0.027	0.078±0.009	0.074±0.010	···	0.012	19
52306	z'	-21.097±0.017	0.075±0.028	0.073±0.009	0.064±0.010	···	0.012	19
				00:31-03:31UT	03:31-09:01UT			
52307	u'	-20.900±0.020	-0.018±0.007	0.486±0.014	0.488±0.012	···	0.022	26
52307	g'	-22.548±0.009	0.038±0.005	0.189±0.006	0.189±0.005	···	0.009	25
52307	r'	-22.511±0.010	-0.067±0.011	0.102±0.006	0.099±0.005	···	0.009	23
52307	i'	-21.995±0.012	-0.023±0.017	0.067±0.006	0.062±0.006	···	0.010	25
52307	z'	-21.101±0.017	0.042±0.026	0.080±0.010	0.081±0.008	···	0.015	27
				00:27-03:27UT	03:27-09:14UT			
52308	u'	-20.906±0.033	-0.035±0.013	0.490±0.021	0.481±0.019	···	0.026	23
52308	g'	-22.566±0.013	0.026±0.006	0.199±0.008	0.188±0.007	···	0.010	22
52308	r'	-22.486±0.017	-0.026±0.017	0.096±0.010	0.087±0.008	···	0.013	22
52308	i'	-22.018±0.021	-0.057±0.026	0.077±0.010	0.063±0.009	···	0.013	25
52308	z'	-21.120±0.027	0.027±0.035	0.099±0.014	0.077±0.012	···	0.017	23
				00:26-03:26UT	03:26-09:05UT			
52309	u'	-20.889±0.018	-0.029±0.006	0.455±0.012	0.461±0.012	···	0.020	30
52309	g'	-22.557±0.009	0.036±0.005	0.178±0.006	0.182±0.006	···	0.010	32
52309	r'	-22.505±0.011	-0.054±0.013	0.085±0.007	0.085±0.007	···	0.012	31
52309	i'	-22.004±0.008	-0.030±0.011	0.050±0.005	0.050±0.004	···	0.007	29
52309	z'	-21.092±0.010	0.062±0.015	0.045±0.006	0.052±0.005	···	0.010	31
				00:36-03:36UT	03:36-09:14UT			
52310	u'	-20.931±0.038	-0.054±0.012	0.489±0.027	0.495±0.026	···	0.033	19
52310	g'	-22.538±0.022	0.034±0.011	0.175±0.013	0.173±0.012	···	0.015	18

Table 4—Continued

MJD (1)	Filter (2)	Zeropoint (a) (3)	Instr. Color (b) (4)	1st-Order Ext. (k) block 0 (5)	block 1 (6)	block 2 (7)	Std. rms (mag) (8)	# Std. stars (9)
52310	r'	-22.505±0.010	-0.086±0.010	0.087±0.006	0.087±0.006	···	0.008	19
52310	i'	-22.018±0.024	-0.042±0.032	0.061±0.013	0.062±0.012	···	0.016	20
52310	z'	-21.116±0.029	-0.002±0.037	0.051±0.016	0.050±0.015	···	0.019	21
				00:30-03:30UT	03:30-09:26UT			
52311	u'	-20.929±0.035	-0.051±0.010	0.533±0.025	0.557±0.024	···	0.036	25
52311	g'	-22.547±0.020	0.024±0.009	0.197±0.012	0.220±0.011	···	0.017	25
52311	r'	-22.514±0.018	-0.081±0.016	0.104±0.011	0.128±0.010	···	0.016	26
52311	i'	-22.024±0.019	-0.079±0.022	0.076±0.011	0.095±0.010	···	0.015	25
52311	z'	-21.092±0.019	0.044±0.022	0.075±0.011	0.092±0.010	···	0.015	25
				00:20-03:20UT	03:20-09:06UT			
52312	u'	-20.847±0.032	-0.041±0.011	0.508±0.019	0.477±0.024	···	0.027	22
52312	g'	-22.504±0.022	0.017±0.012	0.191±0.012	0.177±0.013	···	0.019	28
52312	r'	-22.494±0.021	-0.080±0.022	0.114±0.011	0.106±0.012	···	0.019	29
52312	i'	-21.990±0.019	-0.079±0.027	0.076±0.009	0.063±0.010	···	0.015	28
52312	z'	-21.059±0.027	0.009±0.037	0.074±0.012	0.051±0.014	···	0.020	27
				02:32-04:05UT				
52424	u'	-20.816±0.050	-0.058±0.012	0.466±0.029	···	···	0.026	9
52424	g'	-22.391±0.030	0.029±0.015	0.138±0.017	···	···	0.015	9
52424	r'	-22.420±0.026	-0.051±0.025	0.070±0.014	···	···	0.013	9
52424	i'	-21.936±0.011	-0.008±0.014	0.036±0.006	···	···	0.005	8
52424	z'	-21.028±0.026	0.108±0.033	0.034±0.014	···	···	0.013	9
				01:20-04:20UT	04:20-09:27UT			
52552	u'	-20.791±0.012	-0.027±0.004	0.464±0.008	0.461±0.009	···	0.015	43
52552	g'	-22.444±0.007	0.031±0.004	0.166±0.005	0.162±0.005	···	0.008	41
52552	r'	-22.424±0.007	-0.028±0.007	0.090±0.004	0.083±0.005	···	0.008	42
52552	i'	-21.953±0.009	-0.023±0.016	0.049±0.006	0.042±0.007	···	0.011	43
52552	z'	-21.087±0.010	0.041±0.016	0.043±0.006	0.039±0.007	···	0.011	43
				00:19-03:19UT	03:19-07:21UT			
52553	u'	-20.778±0.016	-0.029±0.007	0.466±0.012	0.470±0.010	···	0.020	37
52553	g'	-22.442±0.012	0.026±0.007	0.168±0.008	0.167±0.007	···	0.013	37
52553	r'	-22.440±0.016	-0.055±0.018	0.098±0.012	0.094±0.010	···	0.018	39
52553	i'	-21.952±0.009	-0.025±0.017	0.055±0.006	0.049±0.005	···	0.010	37
52553	z'	-21.088±0.011	0.022±0.020	0.052±0.007	0.040±0.006	···	0.012	37
				23:49-02:49UT	02:49-05:49UT	05:49-09:25UT		
52554	u'	-20.776±0.024	-0.031±0.008	0.464±0.019	0.470±0.017	0.462±0.017	0.025	37
52554	g'	-22.448±0.012	0.019±0.006	0.169±0.009	0.160±0.008	0.159±0.009	0.012	37
52554	r'	-22.427±0.017	-0.043±0.017	0.083±0.013	0.085±0.012	0.082±0.012	0.018	38

Table 4—Continued

MJD	Filter	Zeropoint (a)	Instr. Color (b)	1st-Order Ext. (k)			Std. rms	# Std.
				block 0	block 1	block 2	(mag)	stars
(1)	(2)	(3)	(4)	(5)	(6)	(7)	(8)	(9)
52554	i'	-21.943±0.012	-0.010±0.019	0.044±0.008	0.034±0.008	0.041±0.008	0.011	34
52554	z'	-21.100±0.012	-0.013±0.020	0.032±0.009	0.022±0.008	0.028±0.008	0.011	34
				23:54-02:54UT	02:54-05:54UT	05:54-09:25UT		
52555	u'	-20.785±0.024	-0.036±0.010	0.442±0.018	0.483±0.018	0.461±0.017	0.023	32
52555	g'	-22.451±0.017	0.025±0.009	0.158±0.013	0.175±0.012	0.161±0.012	0.016	33
52555	r'	-22.426±0.015	-0.026±0.014	0.085±0.011	0.089±0.011	0.085±0.010	0.014	33
52555	i'	-21.951±0.010	0.003±0.014	0.048±0.007	0.047±0.007	0.049±0.007	0.009	31
52555	z'	-21.100±0.018	0.029±0.025	0.035±0.013	0.040±0.012	0.033±0.012	0.016	33
				23:51-02:51UT	02:51-05:51UT	05:51-09:12UT		
52556	u'	-20.752±0.015	-0.035±0.009	0.433±0.011	0.450±0.009	0.463±0.011	0.019	37
52556	g'	-22.461±0.011	0.007±0.008	0.158±0.008	0.167±0.007	0.166±0.008	0.013	37
52556	r'	-22.433±0.007	-0.055±0.011	0.086±0.005	0.086±0.004	0.086±0.005	0.008	34
52556	i'	-21.963±0.009	-0.037±0.018	0.050±0.005	0.047±0.005	0.049±0.005	0.009	35
52556	z'	-21.109±0.013	0.005±0.027	0.037±0.008	0.043±0.007	0.037±0.009	0.014	36
				23:46-02:46UT	02:46-05:46UT	05:46-08:50UT		
52557	u'	-20.783±0.019	-0.038±0.006	0.455±0.014	0.492±0.016	0.483±0.014	0.017	34
52557	g'	-22.460±0.012	0.010±0.007	0.168±0.010	0.180±0.011	0.173±0.010	0.012	34
52557	r'	-22.412±0.014	-0.039±0.014	0.081±0.011	0.086±0.013	0.084±0.011	0.014	35
52557	i'	-21.950±0.011	-0.038±0.017	0.052±0.008	0.056±0.009	0.053±0.008	0.010	32
52557	z'	-21.066±0.012	0.010±0.019	0.028±0.009	0.041±0.011	0.043±0.009	0.011	34
				23:56-02:56UT	02:56-05:56UT	05:56-09:25UT		
52558	u'	-20.828±0.022	-0.029±0.008	0.519±0.016	0.527±0.017	0.515±0.017	0.025	41
52558	g'	-22.430±0.011	0.026±0.006	0.170±0.008	0.170±0.008	0.162±0.009	0.013	40
52558	r'	-22.421±0.012	-0.037±0.011	0.094±0.008	0.092±0.008	0.092±0.008	0.011	36
52558	i'	-21.949±0.007	-0.031±0.012	0.053±0.005	0.050±0.006	0.050±0.006	0.008	38
52558	z'	-21.089±0.010	0.032±0.017	0.052±0.007	0.054±0.007	0.047±0.008	0.011	39
				01:07-09:07UT				
52680	u'	-20.806±0.048	-0.013±0.015	0.606±0.035	···	···	0.023	8
52680	g'	-22.367±0.054	0.046±0.036	0.252±0.033	···	···	0.022	9
52680	r'	-22.330±0.053	0.016±0.084	0.128±0.030	···	···	0.021	10
52680	i'	-21.893±0.047	0.003±0.091	0.092±0.026	···	···	0.017	9
52680	z'	-21.008±0.059	0.065±0.116	0.069±0.033	···	···	0.021	9
				00:40-03:40UT	03:40-09:25UT			
52681	u'	-20.751±0.023	-0.049±0.009	0.547±0.015	0.531±0.014	···	0.021	26
52681	g'	-22.369±0.010	0.019±0.005	0.203±0.005	0.208±0.005	···	0.008	24
52681	r'	-22.362±0.009	-0.040±0.010	0.110±0.005	0.113±0.005	···	0.008	26
52681	i'	-21.905±0.011	-0.029±0.017	0.076±0.005	0.077±0.005	···	0.008	25

Table 4—Continued

MJD	Filter	Zeropoint (a)	Instr. Color (b)	1st-Order Ext. (k)			Std. rms	# Std.
				block 0	block 1	block 2	(mag)	stars
(1)	(2)	(3)	(4)	(5)	(6)	(7)	(8)	(9)
52681	z'	-21.043±0.018	0.049±0.027	0.083±0.009	0.078±0.009	···	0.013	26
				00:40-04:13UT				
52682	u'	-20.749±0.015	-0.026±0.008	0.555±0.010	···	···	0.013	12
52682	g'	-22.383±0.011	0.024±0.007	0.223±0.006	···	···	0.008	12
52682	r'	-22.383±0.012	-0.025±0.015	0.133±0.006	···	···	0.008	12
52682	i'	-21.931±0.011	-0.049±0.022	0.091±0.005	···	···	0.006	12
52682	z'	-21.029±0.027	0.036±0.059	0.080±0.010	···	···	0.014	9
				00:44-03:44UT	03:44-08:41UT			
52683	u'	-20.725±0.025	-0.044±0.008	0.522±0.016	0.501±0.019	···	0.022	21
52683	g'	-22.372±0.013	0.025±0.006	0.201±0.007	0.203±0.009	···	0.010	21
52683	r'	-22.379±0.010	-0.056±0.009	0.110±0.005	0.115±0.006	···	0.007	21
52683	i'	-21.908±0.012	-0.041±0.016	0.066±0.006	0.080±0.007	···	0.008	21
52683	z'	-21.021±0.018	0.047±0.023	0.056±0.008	0.075±0.011	···	0.012	21
				00:36-03:36UT	03:36-09:25UT			
52684	u'	-20.709±0.023	-0.036±0.008	0.512±0.015	0.512±0.017	···	0.022	23
52684	g'	-22.367±0.012	0.024±0.007	0.190±0.007	0.201±0.007	···	0.011	24
52684	r'	-22.381±0.014	-0.073±0.015	0.106±0.008	0.113±0.009	···	0.012	23
52684	i'	-21.912±0.012	-0.046±0.020	0.075±0.006	0.086±0.007	···	0.010	24
52684	z'	-20.982±0.020	0.020±0.027	0.049±0.013	0.063±0.012	···	0.013	20
				00:25-03:25UT	03:25-06:25UT	06:25-09:28UT		
52685	u'	-20.702±0.021	-0.028±0.008	0.516±0.014	0.516±0.017	0.483±0.015	0.021	23
52685	g'	-22.361±0.006	0.032±0.003	0.193±0.003	0.201±0.004	0.199±0.003	0.004	21
52685	r'	-22.374±0.018	-0.044±0.019	0.109±0.009	0.115±0.012	0.108±0.010	0.013	20
52685	i'	-21.906±0.007	-0.047±0.010	0.070±0.004	0.076±0.004	0.075±0.004	0.005	21
52685	z'	-21.010±0.018	0.016±0.026	0.063±0.009	0.064±0.011	0.051±0.009	0.013	23
				00:31-03:31UT	03:31-09:27UT			
52686	u'	-20.720±0.023	-0.044±0.009	0.508±0.015	0.488±0.015	···	0.020	22
52686	g'	-22.354±0.014	0.030±0.006	0.182±0.007	0.174±0.007	···	0.009	23
52686	r'	-22.347±0.019	-0.039±0.017	0.089±0.010	0.085±0.011	···	0.012	20
52686	i'	-21.904±0.019	-0.035±0.027	0.061±0.009	0.059±0.009	···	0.012	23
52686	z'	-21.031±0.035	0.015±0.050	0.054±0.016	0.038±0.017	···	0.023	23
				22:59-01:59UT	01:59-04:59UT	04:59-10:43UT		
52840	u'	-20.682±0.017	-0.034±0.008	0.465±0.012	0.468±0.013	0.478±0.012	0.019	44
52840	g'	-22.322±0.008	0.022±0.006	0.166±0.005	0.164±0.006	0.166±0.005	0.009	45
52840	r'	-22.323±0.008	-0.031±0.011	0.094±0.005	0.094±0.005	0.086±0.005	0.008	43
52840	i'	-21.838±0.013	0.007±0.027	0.049±0.007	0.048±0.007	0.048±0.007	0.011	42
52840	z'	-20.997±0.014	0.063±0.031	0.056±0.008	0.055±0.009	0.056±0.008	0.014	44

Table 4—Continued

MJD	Filter	Zeropoint (a)	Instr. Color (b)	1st-Order Ext. (k)			Std. rms	# Std.
				block 0	block 1	block 2	(mag)	stars
(1)	(2)	(3)	(4)	(5)	(6)	(7)	(8)	(9)
				01:24-04:24UT	04:24-08:59UT			
53031	u'	-20.511±0.022	-0.047±0.008	0.487±0.013	0.465±0.016	···	0.027	30
53031	g'	-22.172±0.011	0.026±0.006	0.171±0.005	0.159±0.007	···	0.010	29
53031	r'	-22.193±0.014	-0.039±0.015	0.093±0.007	0.086±0.008	···	0.013	31
53031	i'	-21.741±0.012	-0.034±0.019	0.066±0.006	0.056±0.007	···	0.012	31
53031	z'	-20.858±0.021	0.024±0.033	0.069±0.010	0.044±0.012	···	0.020	31
				00:47-03:47UT	03:47-09:26UT			
53032	u'	-20.531±0.029	-0.040±0.015	0.465±0.020	0.472±0.020	···	0.036	27
53032	g'	-22.203±0.010	0.020±0.007	0.156±0.006	0.165±0.006	···	0.011	27
53032	r'	-22.225±0.009	-0.056±0.011	0.082±0.005	0.088±0.005	···	0.008	27
53032	i'	-21.774±0.011	-0.064±0.019	0.048±0.005	0.057±0.005	···	0.010	26
53032	z'	-20.908±0.022	0.008±0.039	0.044±0.011	0.052±0.011	···	0.020	26
				00:43-03:43UT	03:43-08:56UT			
53033	u'	-20.560±0.020	-0.031±0.007	0.502±0.013	0.474±0.015	···	0.022	30
53033	g'	-22.225±0.008	0.028±0.004	0.188±0.005	0.173±0.005	···	0.008	31
53033	r'	-22.245±0.010	-0.046±0.012	0.109±0.006	0.095±0.007	···	0.011	32
53033	i'	-21.767±0.008	-0.023±0.014	0.069±0.004	0.057±0.005	···	0.008	30
53033	z'	-20.907±0.015	0.060±0.028	0.082±0.009	0.060±0.010	···	0.015	30
				00:42-03:12UT	03:12-05:42UT	05:42-08:59UT		
53034	u'	-20.555±0.017	-0.036±0.006	0.492±0.012	0.482±0.012	0.498±0.014	0.020	33
53034	g'	-22.223±0.012	0.027±0.006	0.178±0.007	0.176±0.007	0.201±0.008	0.012	33
53034	r'	-22.250±0.014	-0.054±0.014	0.103±0.008	0.103±0.008	0.126±0.009	0.013	31
53034	i'	-21.790±0.012	-0.049±0.016	0.066±0.007	0.066±0.007	0.087±0.008	0.011	33
53034	z'	-20.937±0.017	0.019±0.025	0.074±0.009	0.073±0.009	0.097±0.010	0.016	34
				00:40-03:40UT	03:40-09:06UT			
53035	u'	-20.562±0.023	-0.042±0.007	0.514±0.015	0.493±0.016	···	0.028	36
53035	g'	-22.212±0.007	0.030±0.003	0.183±0.004	0.180±0.004	···	0.007	35
53035	r'	-22.227±0.011	-0.048±0.010	0.101±0.006	0.099±0.006	···	0.011	37
53035	i'	-21.787±0.010	-0.063±0.013	0.078±0.005	0.073±0.005	···	0.009	37
53035	z'	-20.939±0.018	-0.003±0.023	0.095±0.009	0.081±0.010	···	0.017	37
				00:39-03:39UT	03:39-09:09UT			
53036	u'	-20.570±0.015	0.002±0.008	0.507±0.010	0.514±0.011	···	0.019	32
53036	g'	-22.229±0.011	0.030±0.006	0.182±0.006	0.200±0.006	···	0.011	36
53036	r'	-22.261±0.012	-0.048±0.013	0.113±0.006	0.127±0.006	···	0.011	36
53036	i'	-21.798±0.014	-0.016±0.024	0.078±0.006	0.096±0.007	···	0.012	35
53036	z'	-20.960±0.021	0.043±0.037	0.090±0.010	0.117±0.011	···	0.018	34

Table 4—Continued

MJD	Filter	Zeropoint (a)	Instr. Color (b)	1st-Order Ext. (k)			Std. rms	# Std.
				block 0	block 1	block 2	(mag)	stars
(1)	(2)	(3)	(4)	(5)	(6)	(7)	(8)	(9)
				00:38-03:38UT	03:38-08:20UT			
53037	u'	-20.569±0.016	-0.050±0.005	0.506±0.010	0.492±0.011	···	0.018	25
53037	g'	-22.232±0.008	0.017±0.004	0.178±0.004	0.185±0.004	···	0.006	23
53037	r'	-22.248±0.010	-0.089±0.008	0.095±0.005	0.103±0.005	···	0.008	24
53037	i'	-21.783±0.007	-0.072±0.009	0.057±0.004	0.064±0.004	···	0.006	24
53037	z'	-20.925±0.018	0.009±0.021	0.059±0.008	0.064±0.009	···	0.012	23
				23:06-02:06UT	02:06-05:06UT	05:06-10:23UT		
53132	u'	-20.540±0.017	-0.050±0.006	0.508±0.011	0.517±0.012	0.502±0.013	0.019	38
53132	g'	-22.174±0.009	0.024±0.005	0.171±0.005	0.176±0.006	0.171±0.006	0.009	39
53132	r'	-22.186±0.009	-0.049±0.009	0.083±0.005	0.088±0.006	0.085±0.006	0.009	39
53132	i'	-21.708±0.010	-0.025±0.014	0.047±0.005	0.049±0.006	0.043±0.006	0.009	39
53132	z'	-20.838±0.014	0.040±0.019	0.040±0.007	0.037±0.008	0.032±0.009	0.013	39
				23:17-02:17UT	02:17-05:17UT	05:17-10:27UT		
53133	u'	-20.524±0.021	-0.052±0.008	0.503±0.014	0.518±0.016	0.496±0.016	0.022	34
53133	g'	-22.180±0.010	0.021±0.006	0.174±0.006	0.185±0.007	0.177±0.007	0.010	36
53133	r'	-22.180±0.009	-0.046±0.009	0.085±0.005	0.095±0.006	0.086±0.006	0.008	34
53133	i'	-21.710±0.016	-0.043±0.023	0.042±0.008	0.047±0.010	0.044±0.010	0.014	35
53133	z'	-20.860±0.012	0.011±0.017	0.042±0.006	0.053±0.008	0.042±0.007	0.010	34
				23:11-02:11UT	02:11-07:08UT			
53134	u'	-20.517±0.034	-0.040±0.011	0.499±0.022	0.503±0.025	···	0.034	23
53134	g'	-22.168±0.014	0.018±0.008	0.166±0.009	0.161±0.010	···	0.014	25
53134	r'	-22.198±0.009	-0.070±0.010	0.088±0.006	0.086±0.006	···	0.010	26
53134	i'	-21.721±0.009	-0.048±0.014	0.051±0.005	0.051±0.006	···	0.009	26
53134	z'	-20.868±0.015	0.022±0.023	0.045±0.008	0.041±0.010	···	0.015	25
				22:54-01:54UT	01:54-04:54UT	04:54-10:34UT		
53137	u'	-20.507±0.017	-0.045±0.006	0.483±0.010	0.479±0.013	0.481±0.013	0.017	36
53137	g'	-22.162±0.012	0.022±0.006	0.162±0.006	0.166±0.008	0.159±0.008	0.011	37
53137	r'	-22.163±0.011	-0.033±0.011	0.078±0.006	0.074±0.007	0.068±0.008	0.010	36
53137	i'	-21.699±0.018	-0.018±0.024	0.042±0.008	0.046±0.010	0.030±0.010	0.014	33
53137	z'	-20.837±0.021	0.057±0.029	0.044±0.010	0.023±0.012	0.019±0.013	0.017	37
				22:57-01:57UT	01:57-04:57UT	04:57-10:34UT		
53138	u'	-20.527±0.026	-0.012±0.010	0.517±0.021	0.490±0.021	0.505±0.018	0.028	28
53138	g'	-22.178±0.009	0.016±0.005	0.170±0.007	0.164±0.007	0.168±0.006	0.009	27
53138	r'	-22.187±0.009	-0.039±0.009	0.087±0.006	0.091±0.007	0.091±0.006	0.009	28
53138	i'	-21.856±0.010	-0.000±0.026	0.174±0.008	0.156±0.007	0.169±0.001	0.015	22
53138	z'	-20.878±0.011	0.024±0.017	0.042±0.008	0.034±0.008	0.048±0.007	0.011	28
Wt.'ed Mean	u'	-20.792±0.003	-0.034±0.001	0.489±0.002				

Table 4—Continued

MJD	Filter	Zeropoint (a)	Instr. Color (b)	1st-Order Ext. (k)			Std. rms	# Std.
				block 0	block 1	block 2	(mag)	stars
(1)	(2)	(3)	(4)	(5)	(6)	(7)	(8)	(9)
Wt.'ed Mean	g'	-22.433±0.001	0.028±0.001	0.181±0.001				
Wt.'ed Mean	r'	-22.407±0.002	-0.049±0.002	0.095±0.001				
Wt.'ed Mean	i'	-21.934±0.002	-0.037±0.002	0.089±0.001				
Wt.'ed Mean	z'	-21.062±0.002	0.030±0.004	0.053±0.001				

*The second order extinction term values are -2.1×10^{-2}, -1.6×10^{-2}, -4.0×10^{-3}, 6.0×10^{-3} and 3.0×10^{-3}, for the u',g',r',i' and z' respectively. These values are set to the determined coefficients from Smith et al. (2002).

Table 5. The Southern $u'g'r'i'z'$ Secondary Standard Stars

ID	RA (J2000)	DEC (J2000)	u'	$\sigma_{u'}$	$n_{u'}$	g'	$\sigma_{g'}$	$n_{g'}$	r'	$\sigma_{r'}$	$n_{r'}$	i'	$\sigma_{i'}$	$n_{i'}$	z'	$\sigma_{z'}$	$n_{z'}$	$D_{\rm NN}$ (arcsec)	$D_{\rm NN}$ (aperture radii)	Notes[†]
(1)	(2)	(3)	(4)	(5)	(6)	(7)	(8)	(9)	(10)	(11)	(12)	(13)	(14)	(15)	(16)	(17)	(18)	(19)	(20)	(21)
DLS_0520-49																				
ugriz J052015.2-490229	05:20:15.24	-49:02:29.0	12.245	0.002	13	11.103	0.004	8	11.035	0.003	7	11.101	0.003	8	11.170	0.004	9	102.150	13.750	
ugriz J051956.5-490417	05:19:56.58	-49:04:17.4	12.921	0.002	16	11.897	0.001	9	11.627	0.002	9	11.564	0.002	9	11.576	0.002	11	40.790	5.490	
ugriz J051928.0-485735	05:19:28.02	-48:57:35.6	13.312	0.002	17	12.140	0.003	9	11.728	0.002	9	11.593	0.004	10	11.560	0.002	13	9.080	1.220	
ugriz J051949.7-485934	05:19:49.70	-48:59:34.4	14.288	0.003	17	12.554	0.002	12	11.976	0.002	10	11.823	0.001	11	11.765	0.001	13	52.090	7.010	
ugriz J052020.8-485509	05:20:20.80	-48:55:09.1	13.991	0.002	16	12.871	0.003	16	12.528	0.002	14	12.428	0.001	16	12.416	0.002	17	34.770	4.680	
ugriz J051957.1-490625	05:19:57.10	-49:06:25.2	14.331	0.002	15	13.115	0.002	14	12.723	0.002	14	12.601	0.002	14	12.588	0.002	15	33.100	4.450	
ugriz J052029.6-485828	05:20:29.62	-48:58:28.5	15.554	0.003	17	13.712	0.002	17	13.071	0.002	17	12.864	0.002	17	12.774	0.002	17	50.490	6.800	
ugriz J051927.3-485729	05:19:27.38	-48:57:29.1	14.719	0.014	15	13.640	0.015	15	13.335	0.010	15	13.227	0.010	15	13.156	0.008	15	9.080	1.220	
ugriz J051944.4-485737	05:19:44.40	-48:57:37.8	15.127	0.003	16	13.818	0.002	17	13.376	0.002	17	13.251	0.001	17	13.214	0.002	17	35.930	4.840	
ugriz J052040.3-490630	05:20:40.30	-49:06:30.2	15.407	0.010	6	14.153	0.002	6	13.744	0.002	6	13.578	0.003	6	13.545	0.012	6	90.150	12.130	
ugriz J051926.6-490516	05:19:26.65	-49:05:16.4	16.760	0.033	15	14.606	0.005	15	13.833	0.003	15	13.566	0.003	15	13.461	0.003	15	87.600	11.790	
ugriz J052008.4-485455	05:20:08.40	-48:54:55.0	16.132	0.025	17	14.477	0.002	17	13.887	0.002	17	13.694	0.002	17	13.615	0.002	17	58.350	7.850	
ugriz J052036.4-490508	05:20:36.42	-49:05:08.5	15.662	0.010	8	14.603	0.002	8	14.226	0.002	8	14.078	0.003	8	14.054	0.003	8	51.790	6.970	
ugriz J051957.9-490153	05:19:57.97	-49:01:53.4	15.687	0.011	17	14.600	0.002	17	14.271	0.002	17	14.184	0.003	17	14.165	0.007	17	71.050	9.560	
ugriz J051931.3-485751	05:19:31.37	-48:57:51.8	16.647	0.037	16	14.957	0.003	16	14.328	0.003	16	14.099	0.018	16	14.027	0.003	16	26.950	3.630	
ugriz J051954.4-490342	05:19:54.43	-49:03:42.4	17.458	0.019	15	15.255	0.002	17	14.367	0.002	17	14.007	0.002	17	13.823	0.003	17	40.790	5.490	
ugriz J052031.6-490446	05:20:31.65	-49:04:46.5	16.121	0.012	17	14.822	0.002	17	14.389	0.002	17	14.239	0.003	17	14.205	0.004	17	51.790	6.970	
ugriz J051935.5-485548	05:19:35.52	-48:55:48.7	16.769	0.022	17	15.244	0.004	17	14.703	0.003	17	14.533	0.003	17	14.468	0.006	17	98.900	13.310	
ugriz J051936.1-485858	05:19:36.12	-48:58:58.4	16.000	0.018	17	15.136	0.003	17	14.843	0.003	17	14.740	0.003	17	14.712	0.005	17	27.510	3.700	
ugriz J051950.2-490026	05:19:50.22	-49:00:26.2	16.128	0.007	17	15.187	0.002	17	14.864	0.002	17	14.746	0.002	17	14.707	0.005	17	12.020	1.620	
ugriz J052038.7-490242	05:20:38.72	-49:02:42.7	16.643	0.083	10	15.388	0.016	11	14.906	0.018	11	14.696	0.016	10	14.625	0.018	10	142.010	19.110	
ugriz J051944.8-485702	05:19:44.87	-48:57:02.1	16.438	0.019	16	15.335	0.004	17	14.966	0.004	17	14.848	0.004	17	14.829	0.007	17	35.930	4.840	
ugriz J052033.2-485914	05:20:33.27	-48:59:14.6	17.112	0.011	13	15.593	0.004	14	15.048	0.003	15	14.859	0.004	15	14.791	0.006	15	58.450	7.870	
ugriz J051934.9-490359	05:19:34.95	-49:03:59.7	16.398	0.135	17	15.497	0.013	17	15.105	0.009	17	14.970	0.004	17	14.926	0.005	17	42.260	5.690	
ugriz J052016.3-490032	05:20:16.38	-49:00:32.7	17.466	0.023	15	15.780	0.005	16	15.197	0.004	16	15.021	0.004	15	14.916	0.007	15	60.890	8.200	
ugriz J052006.2-490138	05:20:06.23	-49:01:38.2	16.974	0.028	12	15.734	0.007	13	15.249	0.005	13	15.080	0.005	13	15.006	0.006	13	82.640	11.120	
ugriz J051925.6-485321	05:19:25.64	-48:53:21.8	16.863	0.028	13	15.756	0.026	13	15.316	0.019	13	15.121	0.016	13	15.041	0.016	13	144.920	19.500	
ugriz J051944.9-490146	05:19:44.99	-49:01:46.9	18.231	0.073	10	16.339	0.009	17	15.546	0.004	17	15.275	0.006	17	15.143	0.010	17	7.930	1.070	
ugriz J052031.5-485425	05:20:31.57	-48:54:25.9	17.302	0.034	15	16.030	0.004	16	15.602	0.005	16	15.459	0.005	16	15.435	0.007	16	45.760	6.160	
ugriz J051948.1-485625	05:19:48.10	-48:56:25.4	17.209	0.044	16	16.175	0.008	17	15.656	0.005	17	15.450	0.005	17	15.339	0.018	17	26.790	3.610	
ugriz J052027.9-485454	05:20:27.91	-48:54:54.0	18.347	0.036	8	16.430	0.015	17	15.811	0.006	17	15.566	0.006	17	15.466	0.016	17	45.760	6.160	

Table 5—Continued

ID	RA (J2000)	DEC (J2000)	u'	$\sigma_{u'}$	$n_{u'}$	g'	$\sigma_{g'}$	$n_{g'}$	r'	$\sigma_{r'}$	$n_{r'}$	i'	$\sigma_{i'}$	$n_{i'}$	z'	$\sigma_{z'}$	$n_{z'}$	$D_{\rm NN}$ (arcsec)	$D_{\rm NN}$ (aperture radii)	Notes[†]
(1)	(2)	(3)	(4)	(5)	(6)	(7)	(8)	(9)	(10)	(11)	(12)	(13)	(14)	(15)	(16)	(17)	(18)	(19)	(20)	(21)
ugriz J051945.0-490216	05:19:45.01	-49:02:16.0	18.162	0.145	8	16.558	0.010	17	15.836	0.005	17	15.574	0.007	17	15.434	0.017	17	21.240	2.860	
ugriz J052023.4-485532	05:20:23.41	-48:55:32.5	17.246	0.022	16	16.214	0.008	17	15.852	0.007	17	15.703	0.005	17	15.678	0.009	17	34.770	4.680	
ugriz J052012.3-490457	05:20:12.35	-49:04:57.7	17.398	0.020	16	16.287	0.008	17	15.936	0.009	17	15.830	0.013	17	15.807	0.015	16	32.290	4.350	
ugriz J052000.0-490325	05:20:00.03	-49:03:25.5	18.281	0.020	10	16.686	0.014	17	16.068	0.007	17	15.849	0.006	17	15.736	0.016	17	35.650	4.800	
ugriz J051936.1-490518	05:19:36.13	-49:05:18.9	18.832	0.050	5	16.948	0.017	17	16.232	0.006	17	15.973	0.006	17	15.847	0.016	16	80.050	10.770	
ugriz J051938.2-485840	05:19:38.20	-48:58:40.0	18.304	0.118	9	16.851	0.019	17	16.232	0.012	17	16.005	0.013	17	15.915	0.035	17	23.750	3.200	
ugriz J052000.1-485544	05:20:00.17	-48:55:44.7	17.889	0.037	13	16.684	0.011	17	16.239	0.010	17	16.068	0.007	17	16.016	0.013	15	40.650	5.470	
ugriz J051945.0-490154	05:19:45.03	-49:01:54.8	18.599	0.145	7	16.935	0.018	16	16.269	0.016	17	16.023	0.027	17	15.922	0.011	16	7.930	1.070	
ugriz J051936.9-485726	05:19:36.93	-48:57:26.6	18.068	0.056	13	16.821	0.017	17	16.285	0.019	17	16.163	0.007	17	16.134	0.010	13	32.710	4.400	
ugriz J052031.8-490549	05:20:31.89	-49:05:49.2	-100.000	-100.000	0	17.628	0.022	14	16.395	0.010	17	15.741	0.008	17	15.453	0.007	17	60.280	8.110	
ugriz J052015.0-485814	05:20:15.07	-48:58:14.1	-100.000	-100.000	0	17.548	0.035	14	16.403	0.011	17	15.939	0.010	17	15.703	0.006	17	54.950	7.400	
ugriz J051955.2-490259	05:19:55.26	-49:02:59.2	-100.000	-100.000	0	17.650	0.074	13	16.406	0.010	17	15.568	0.005	17	15.180	0.010	17	43.970	5.920	
ugriz J052000.1-490456	05:20:00.12	-49:04:56.2	19.088	-100.000	1	17.366	0.074	15	16.516	0.007	17	16.207	0.013	17	16.024	0.014	14	52.200	7.030	
ugriz J052009.7-490517	05:20:09.78	-49:05:17.8	18.735	0.141	6	17.193	0.020	16	16.535	0.015	17	16.307	0.014	17	16.200	0.018	12	32.290	4.350	
ugriz J051950.7-490139	05:19:50.79	-49:01:39.0	18.827	0.081	5	17.197	0.011	16	16.562	0.011	17	16.340	0.012	17	16.191	0.032	13	57.530	7.740	
ugriz J052033.2-485752	05:20:33.21	-48:57:52.5	18.256	0.084	7	17.068	0.016	12	16.599	0.014	14	16.443	0.014	14	16.377	0.022	6	50.490	6.800	
ugriz J051946.5-490433	05:19:46.59	-49:04:33.9	18.291	0.036	8	17.110	0.019	16	16.636	0.013	17	16.450	0.014	17	16.332	0.050	9	92.630	12.470	
ugriz J051957.9-490553	05:19:57.94	-49:05:53.1	18.330	-100.000	1	17.544	0.015	14	16.642	0.013	17	16.295	0.010	17	16.161	0.014	13	33.100	4.450	
ugriz J051959.2-485505	05:19:59.23	-48:55:05.1	18.334	0.049	10	17.207	0.015	16	16.728	0.012	17	16.527	0.016	17	16.410	0.020	9	32.510	4.380	
ugriz J051918.7-490436	05:19:18.73	-49:04:36.1	18.609	0.101	5	17.449	0.043	12	16.888	0.028	12	16.550	0.025	11	16.445	0.045	6	87.600	11.790	
ugriz J052015.7-485929	05:20:15.74	-48:59:29.0	-100.000	-100.000	0	18.149	0.041	7	16.900	0.011	17	16.178	0.011	17	15.738	0.052	17	4.810	0.650	
ugriz J052016.1-485931	05:20:16.13	-48:59:31.9	-100.000	-100.000	0	18.172	0.028	9	16.914	0.016	17	16.181	0.009	17	15.730	0.047	17	4.810	0.650	
ugriz J051923.9-485545	05:19:23.99	-48:55:45.8	18.888	0.120	5	17.526	0.036	12	16.967	0.018	14	16.696	0.023	13	16.629	0.028	7	108.590	14.610	
ugriz J052002.5-485501	05:20:02.51	-48:55:01.2	-100.000	-100.000	0	18.201	0.022	8	16.973	0.019	17	15.808	0.007	17	15.269	0.008	17	32.510	4.380	
ugriz J051949.9-485605	05:19:49.93	-48:56:05.6	-100.000	-100.000	0	18.209	0.016	9	17.016	0.014	16	16.406	0.023	17	16.090	0.022	14	26.790	3.610	
ugriz J051938.7-490243	05:19:38.75	-49:02:43.4	-100.000	-100.000	0	18.336	0.028	7	17.048	0.024	16	15.998	0.012	17	15.512	0.008	17	42.700	5.750	
ugriz J052010.5-485741	05:20:10.57	-48:57:41.7	-100.000	-100.000	0	18.091	0.042	10	17.110	0.019	16	16.758	0.012	15	16.389	0.109	9	54.950	7.400	
ugriz J052021.0-490615	05:20:21.02	-49:06:15.8	-100.000	-100.000	0	18.581	0.035	5	17.134	0.018	16	16.146	0.011	17	15.732	0.012	17	13.590	1.830	
ugriz J052004.6-485613	05:20:04.61	-48:56:13.5	18.710	0.314	6	17.674	0.025	14	17.174	0.021	15	16.991	0.020	10	16.923	0.027	7	52.380	7.050	
ugriz J051950.5-485739	05:19:50.58	-48:57:39.9	18.650	0.047	7	17.656	0.026	13	17.195	0.020	16	17.020	0.017	10	16.866	0.066	6	7.010	0.940	
ugriz J051933.7-490142	05:19:33.79	-49:01:42.2	18.550	0.093	6	17.650	0.025	14	17.220	0.024	16	17.057	0.023	9	16.740	0.236	7	78.200	10.530	
ugriz J051951.0-485745	05:19:51.04	-48:57:45.3	18.694	0.109	5	17.737	0.031	11	17.302	0.025	15	17.155	0.020	8	17.062	0.033	5	7.010	0.940	

Table 5—Continued

ID	RA (J2000)	DEC (J2000)	u'	$\sigma_{u'}$	$n_{u'}$	g'	$\sigma_{g'}$	$n_{g'}$	r'	$\sigma_{r'}$	$n_{r'}$	i'	$\sigma_{i'}$	$n_{i'}$	z'	$\sigma_{z'}$	$n_{z'}$	$D_{\rm NN}$ (arcsec)	$D_{\rm NN}$ (aperture radii)	Notes[†]
(1)	(2)	(3)	(4)	(5)	(6)	(7)	(8)	(9)	(10)	(11)	(12)	(13)	(14)	(15)	(16)	(17)	(18)	(19)	(20)	(21)
ugriz J051933.8-485739	05:19:33.89	-48:57:39.9	18.579	0.236	2	18.023	0.042	11	17.354	0.018	15	16.877	0.014	14	16.645	0.015	8	5.430	0.730	
ugriz J051945.3-485450	05:19:45.35	-48:54:50.7	-100.000	-100.000	0	18.675	0.034	5	17.390	0.022	15	16.672	0.014	15	16.308	0.032	10	87.440	11.770	
ugriz J051933.5-485735	05:19:33.56	-48:57:35.6	-100.000	-100.000	0	18.125	0.026	6	17.402	0.023	14	16.907	0.018	12	16.666	0.023	8	5.430	0.730	
ugriz J051938.5-490336	05:19:38.53	-49:03:36.3	-100.000	-100.000	0	18.742	0.038	5	17.414	0.016	14	15.984	0.014	17	15.192	0.148	17	15.320	2.060	
ugriz J052005.0-485913	05:20:05.03	-48:59:13.5	-100.000	-100.000	0	18.045	0.023	10	17.427	0.024	14	17.240	0.015	8	17.032	0.020	4	106.540	14.340	
ugriz J051959.3-485628	05:19:59.33	-48:56:28.3	-100.000	-100.000	0	18.092	0.029	12	17.522	0.025	13	17.340	0.039	8	17.150	0.063	3	44.340	5.970	
ugriz J051940.3-485850	05:19:40.38	-48:58:50.1	15.066	-100.000	1	18.758	0.042	4	17.526	0.026	14	16.328	0.009	17	15.795	0.012	17	23.750	3.200	
ugriz J052021.9-490605	05:20:21.90	-49:06:05.4	19.168	0.011	3	18.019	0.031	10	17.564	0.028	12	17.412	0.024	8	-100.000	-100.000	0	13.590	1.830	
ugriz J052022.4-490543	05:20:22.42	-49:05:43.0	-100.000	-100.000	0	18.156	0.036	10	17.672	0.025	12	17.482	0.020	8	-100.000	-100.000	0	22.880	3.080	
ugriz J052003.6-490322	05:20:03.64	-49:03:22.3	19.438	-100.000	1	18.116	0.063	9	17.710	0.026	10	17.631	0.020	6	-100.000	-100.000	0	35.650	4.800	
ugriz J051937.5-490324	05:19:37.55	-49:03:24.4	18.808	0.535	3	18.199	0.012	8	17.761	0.010	10	17.592	0.067	6	-100.000	-100.000	0	15.320	2.060	
ugriz J052025.9-490120	05:20:25.99	-49:01:20.2	-100.000	-100.000	0	18.571	0.073	5	17.905	0.027	7	17.694	0.050	6	-100.000	-100.000	0	105.790	14.240	
ugriz J051951.1-490034	05:19:51.14	-49:00:34.2	-100.000	-100.000	0	18.437	0.067	7	18.065	0.010	7	17.750	0.055	4	-100.000	-100.000	0	12.020	1.620	
ugriz J051926.1-490032	05:19:26.14	-49:00:32.7	-100.000	-100.000	0	19.094	0.072	3	18.208	0.028	5	17.774	0.040	3	-100.000	-100.000	0	102.470	13.790	

[†] An entry with an asterisk ($*$) in this column has a $u' - i'$ color greater than 5; so its u'-band magnitude may require a non-negligible red leak correction ($\gtrsim$ 0.01 mag). See § 3.3 of the text for details.

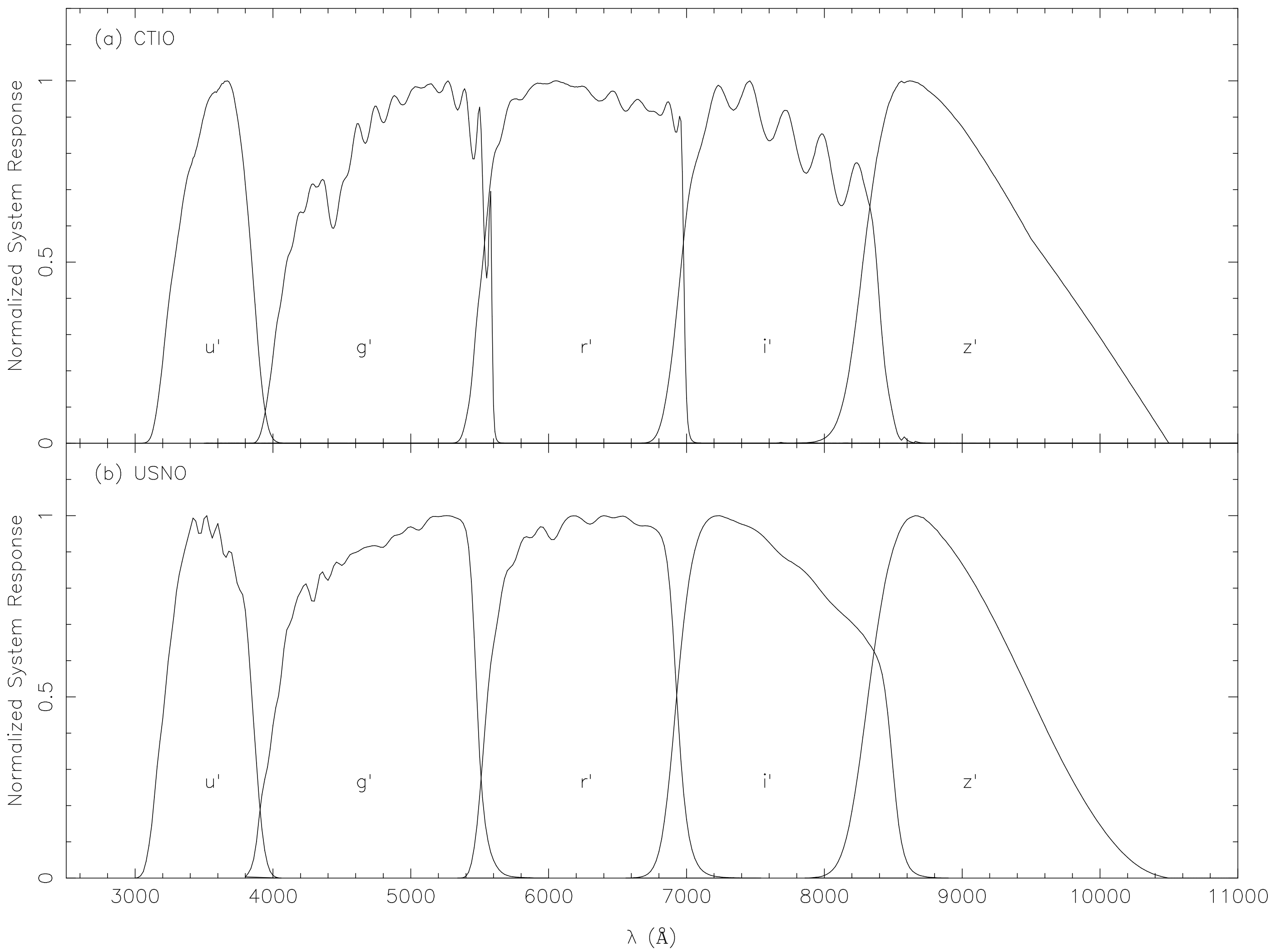

Fig. 1.— The (normalized) responses of the extra-atmospheric $u'g'r'i'z'$ system bandpasses for the (a) CTIO 0.9-m and the (b) USNO 1.0-m telescope systems. The CTIO data should be considered preliminary as the CCD response function was taken from the GIF plot at `http://www.ctio.noao.edu/ccd_info/ccd_info.html` and is approximately ten years old. The filter data are from the manufacturer for an identical filter set to the one used. Note the similarity between the two systems, supported by the low color term values derived in the paper. (Figure 1 of Smith et al. 2003, reproduced by permission by permission of the AAS.)

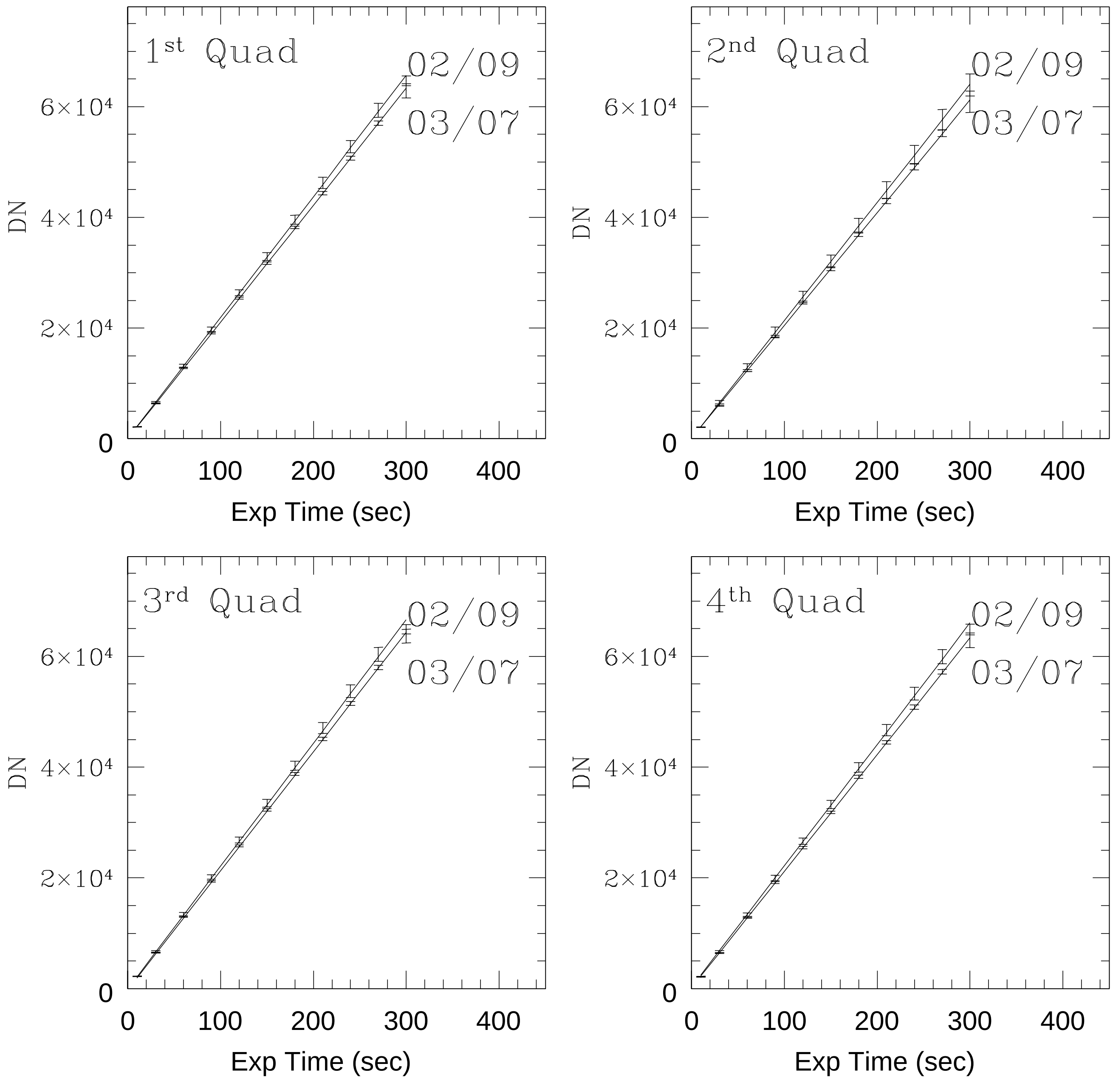

Fig. 2.— Linearity response tests for each quadrant of the Tek2k#3 detector. These show the weighted averages of three independent tests taken during the 2002 September (02/09) and 2003 July (03/07) observing runs. As labeled, the quadrants refer to: 1=LL; 2=UL; 3=LR; and 4=UR as viewed in the default orientation at the telescope (pixel 0,0 in LL; 2048,2048 in UR). The different slopes are due to differences in the illumination of the dome flat screen.

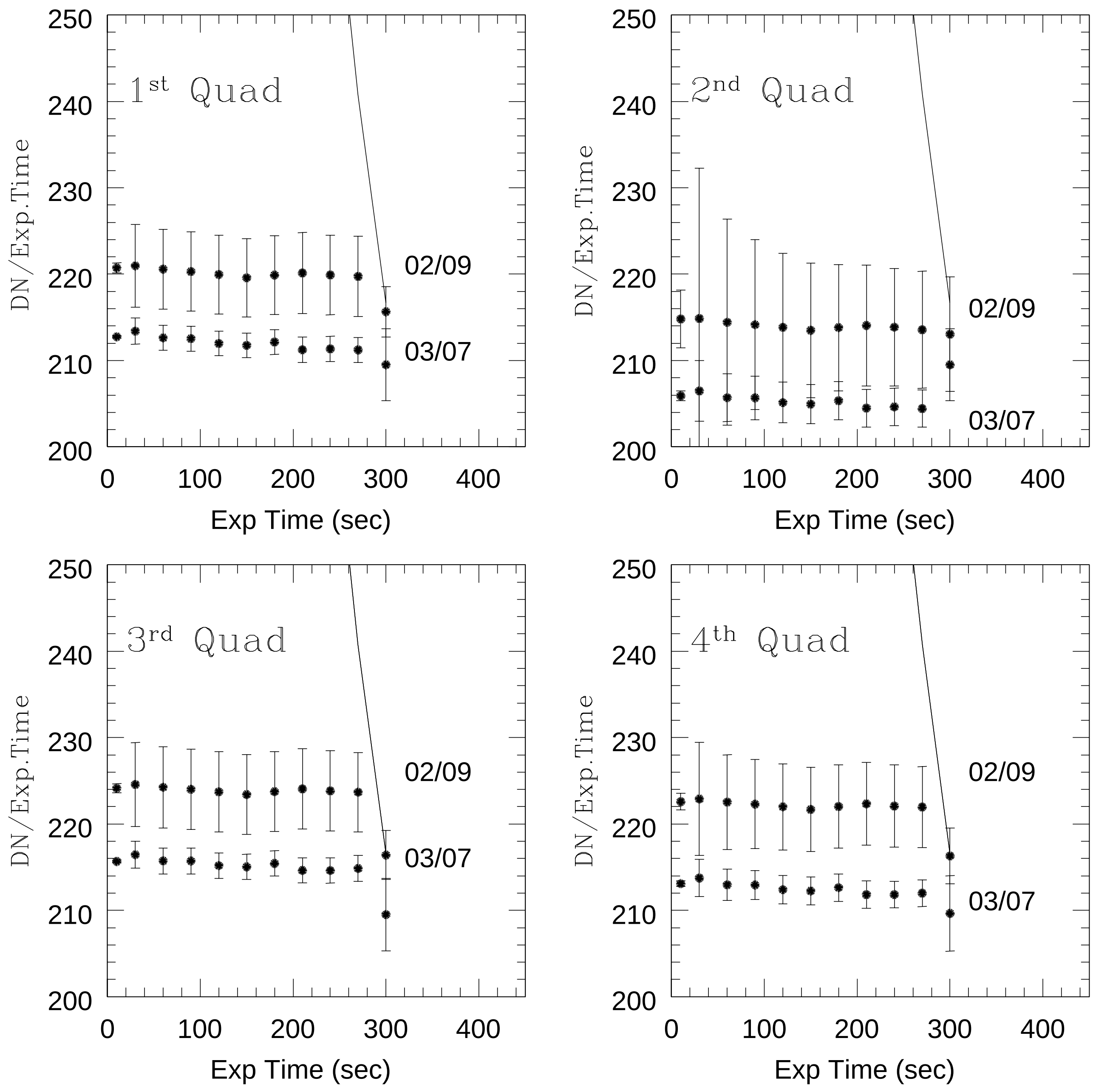

Fig. 3.— Deviation from linearity as a function of exposure time for the CCD. These show the weighted averages for the same three independent tests taken during the September 2002 and July 2003 observing runs. The solid line is the calculated 65,000 DN line. Labeling of the quadrants is the same as in Figure 2.

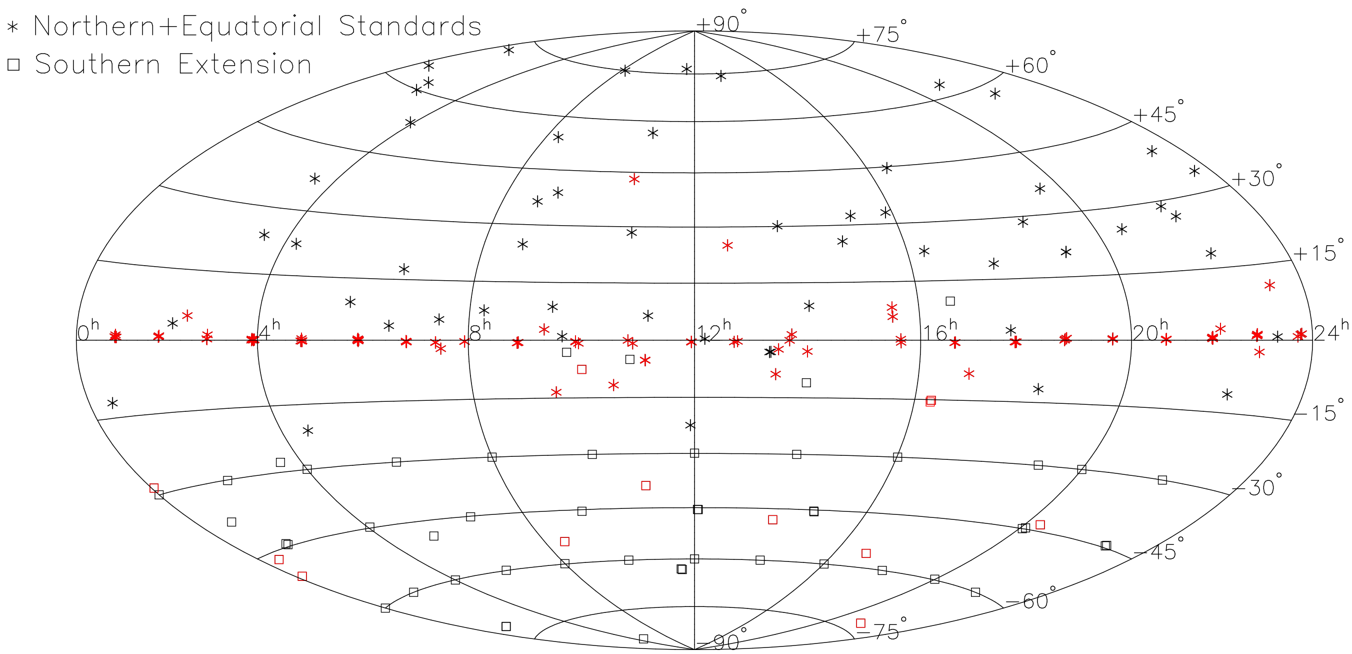

Fig. 4.— Location of all current $u'g'r'i'z'$ standard star fields. The original network fields are shown as asterisks and the new southern extension fields are shown as squares. Fields with complementary $UBVRI$ data from Landolt are shown in red. $UBVRI$ data also exists for the E-region fields at $-45°$ declination.

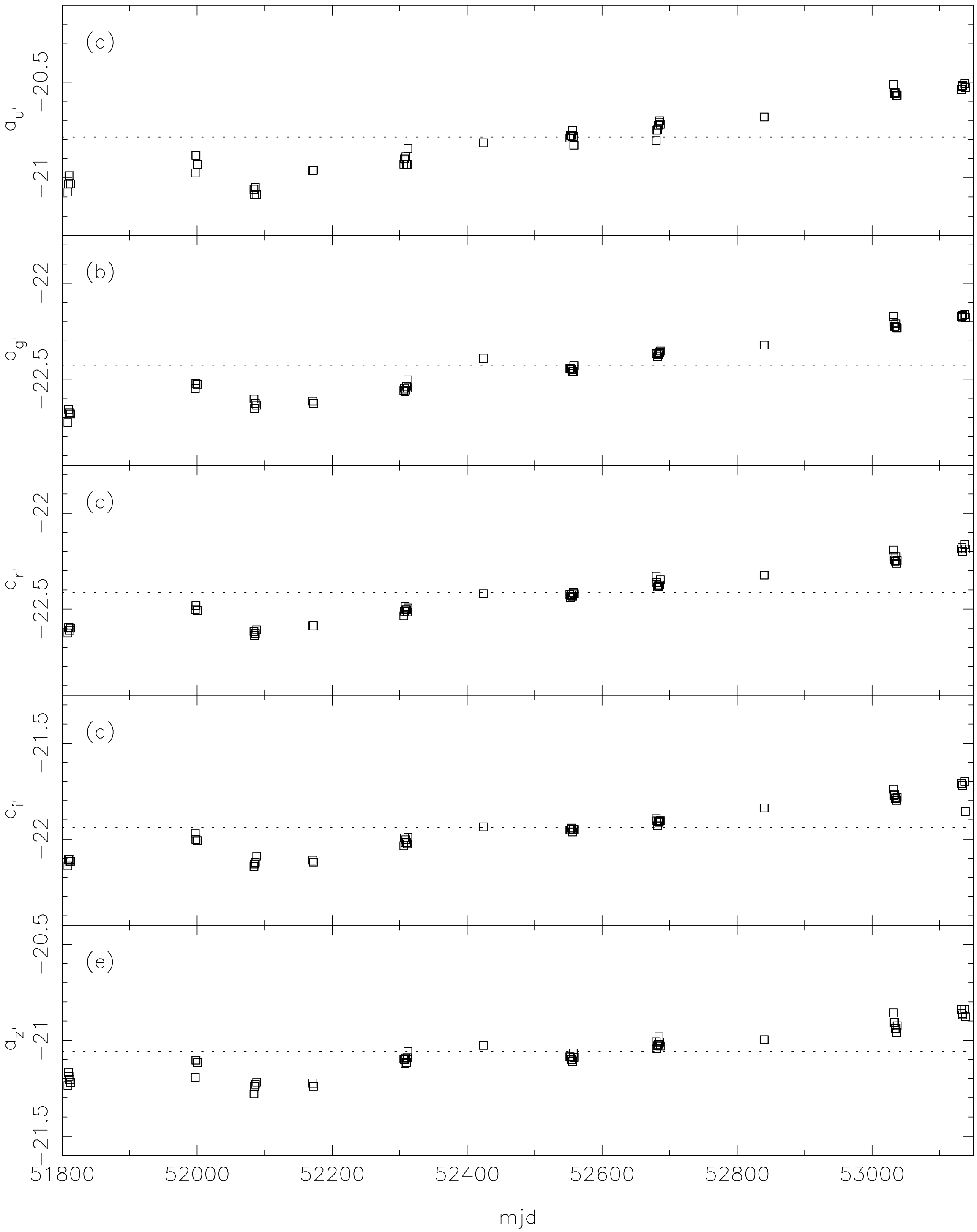

Fig. 5.— The photometric zeropoints for each night of data, by filter, $u'g'r'i'z'$, from top to bottom. The dotted line indicates the (unweighted) mean zeropoints. Note the slight degradation of telescope throughput with time. These values were taken from Table 4.

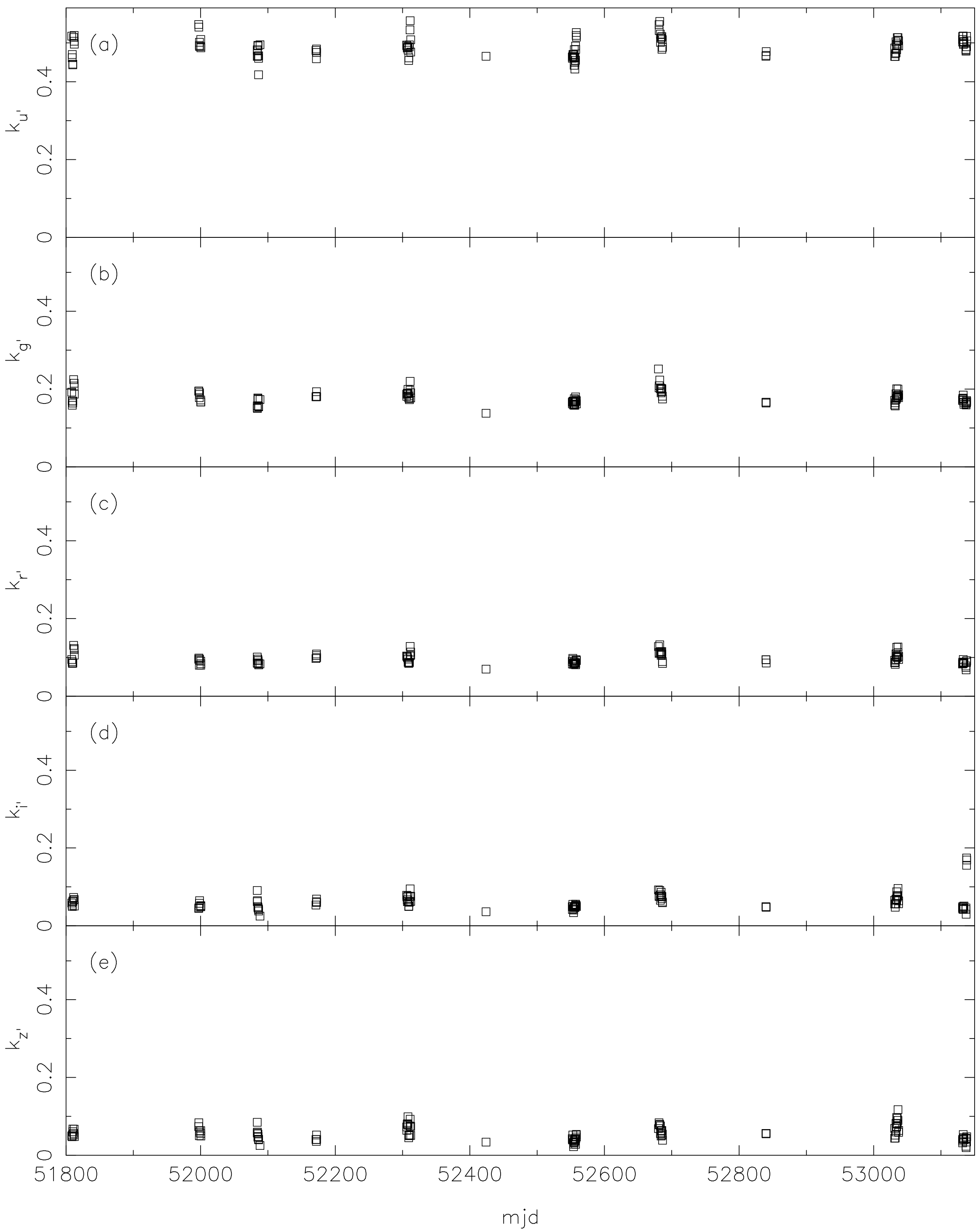

Fig. 6.— The first order extinction coefficients for each reduction block by filter, $u'g'r'i'z'$, from top to bottom. These values were taken from Table 4.

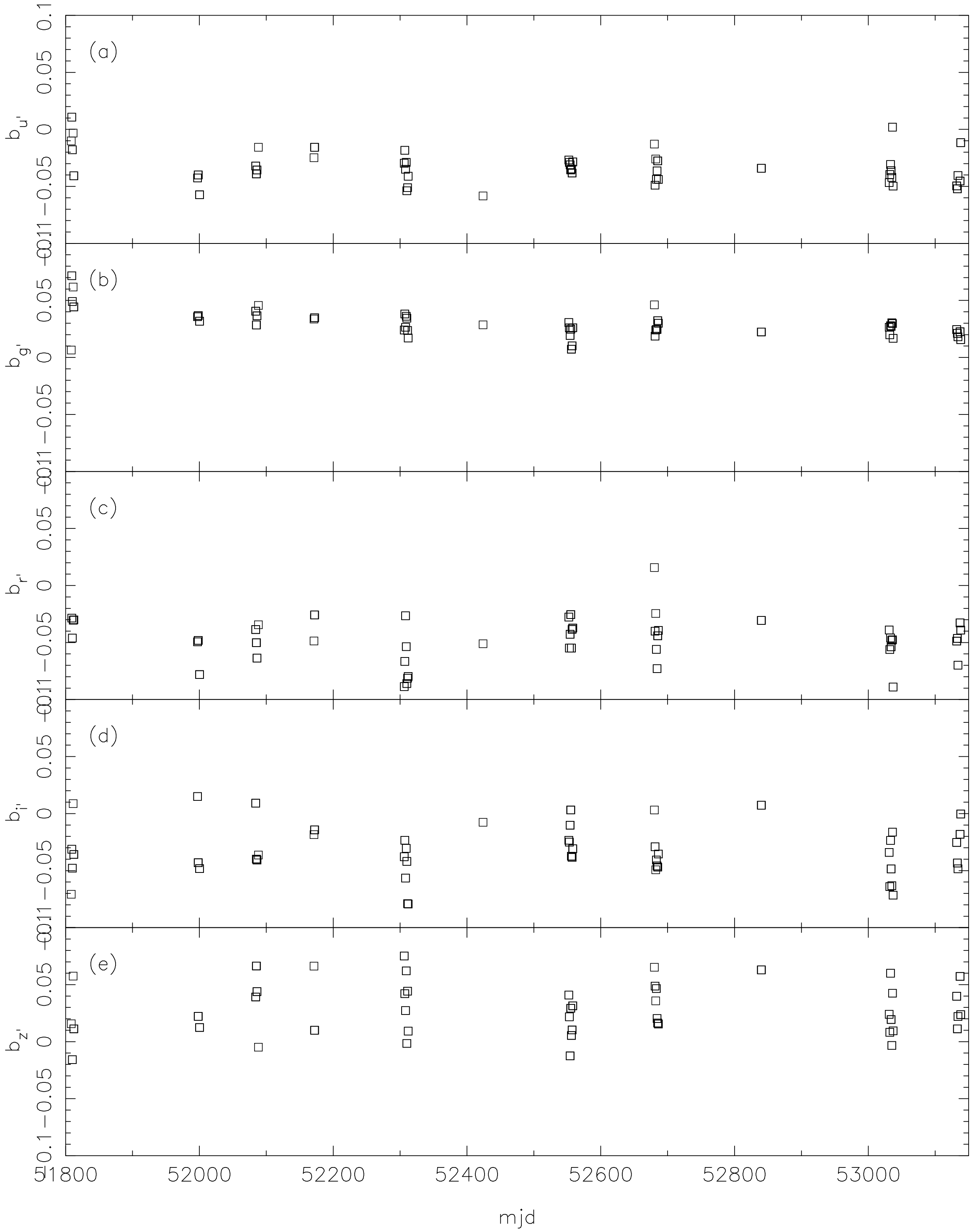

Fig. 7.— The first order color term coefficients for each reduction block by filter, $u'g'r'i'z'$, from top to bottom. These values were taken from Table 4.

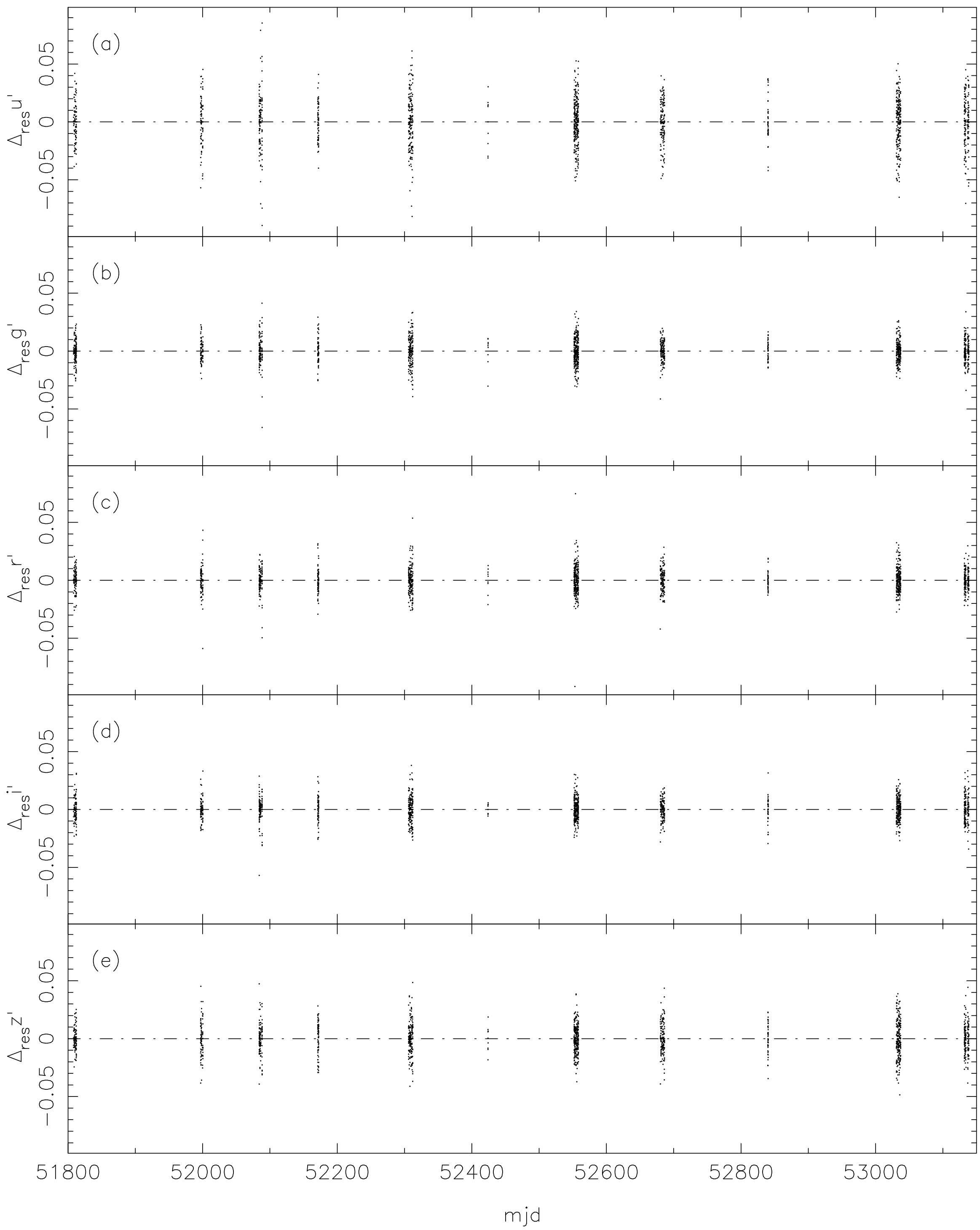

Fig. 8.— The residuals from the `excal` solutions for the Smith et al. (2002) standards plotted as a function of Modified Julian Date (MJD) for all the nights containing photometric data.

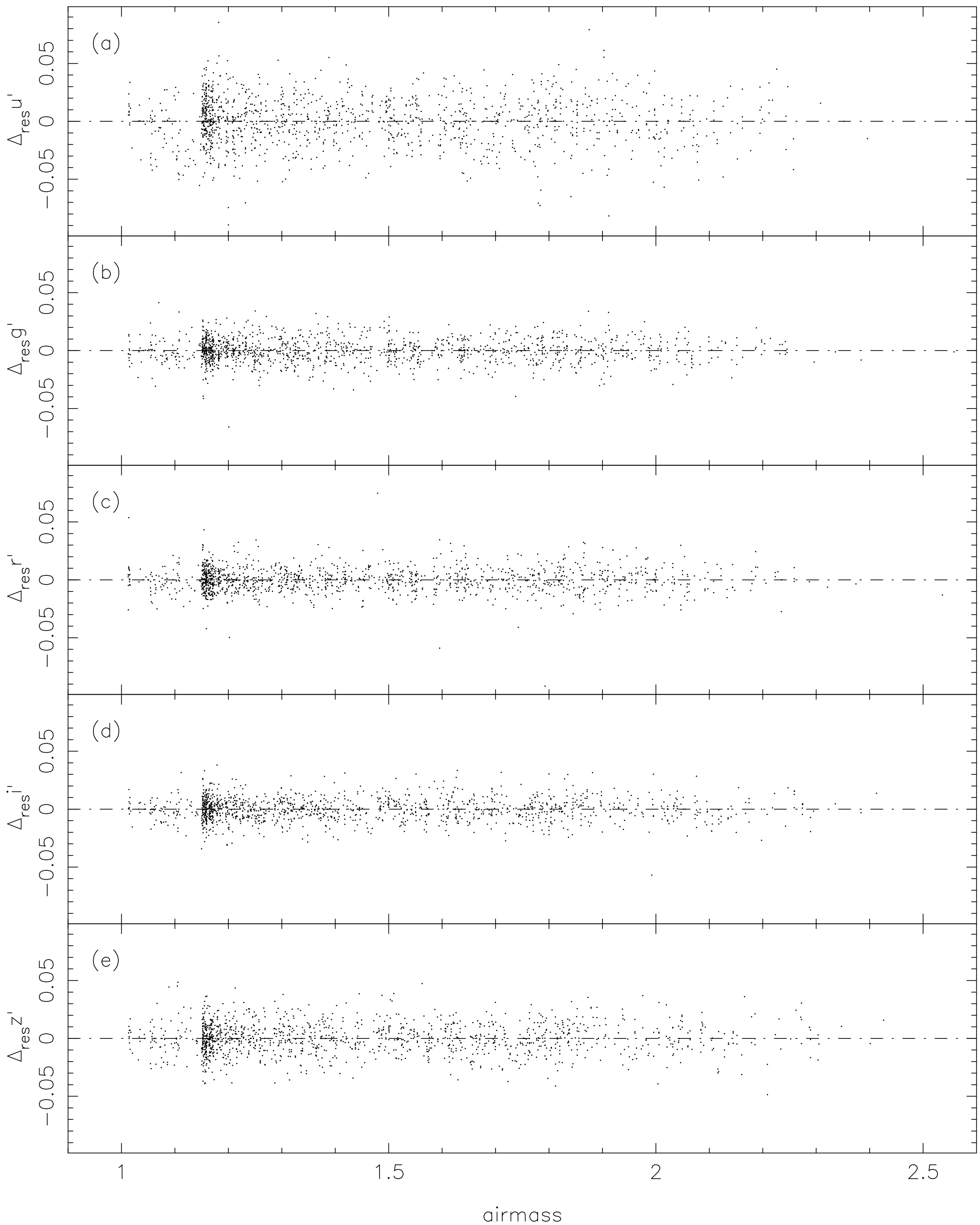

Fig. 9.— The residuals from the `excal` solutions for the Smith et al. (2002) standards plotted as a function of airmass (X) for all the nights containing photometric data.

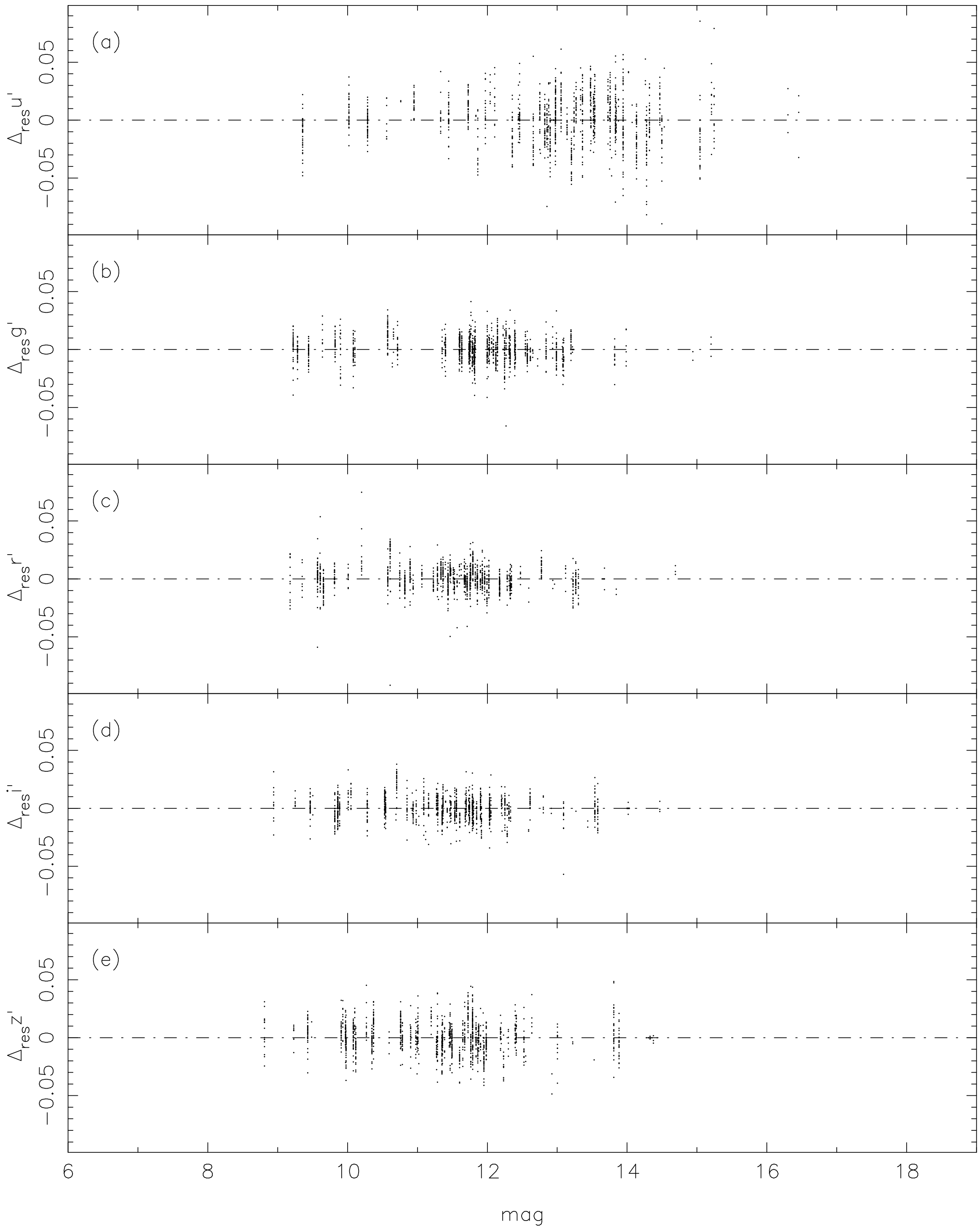

Fig. 10.— The residuals from the `excal` solutions for the Smith et al. (2002) standards plotted as a function of magnitude for all the nights containing photometric data ($\Delta_{\rm res}u'$ vs. u', $\Delta_{\rm res}g'$ vs. g', $\Delta_{\rm res}r'$ vs. r', $\Delta_{\rm res}i'$ vs. i', $\Delta_{\rm res}z'$ vs. z').

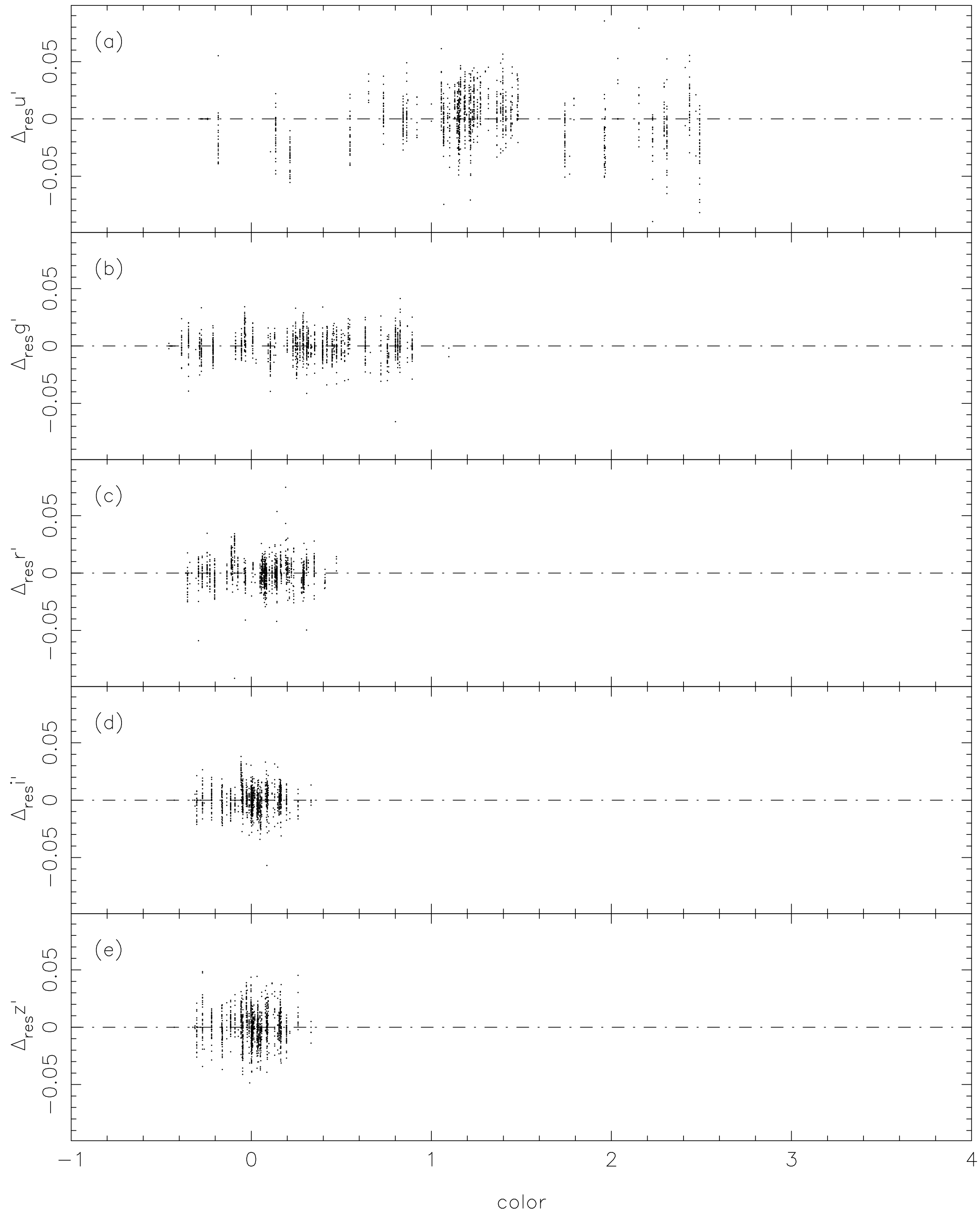

Fig. 11.— The residuals from the `excal` solutions for the Smith et al. (2002) standards plotted as a function of color for all the nights containing photometric data ($\Delta_{\rm res}u'$ vs. $(u'-g')$, $\Delta_{\rm res}g'$ vs. $(g'-r')$, $\Delta_{\rm res}r'$ vs. $(r'-i')$, $\Delta_{\rm res}i'$ vs. $(i'-z')$, $\Delta_{\rm res}z'$ vs. $(i'-z')$). These are plotted in the sense of (observed−standard) for each night's solution.

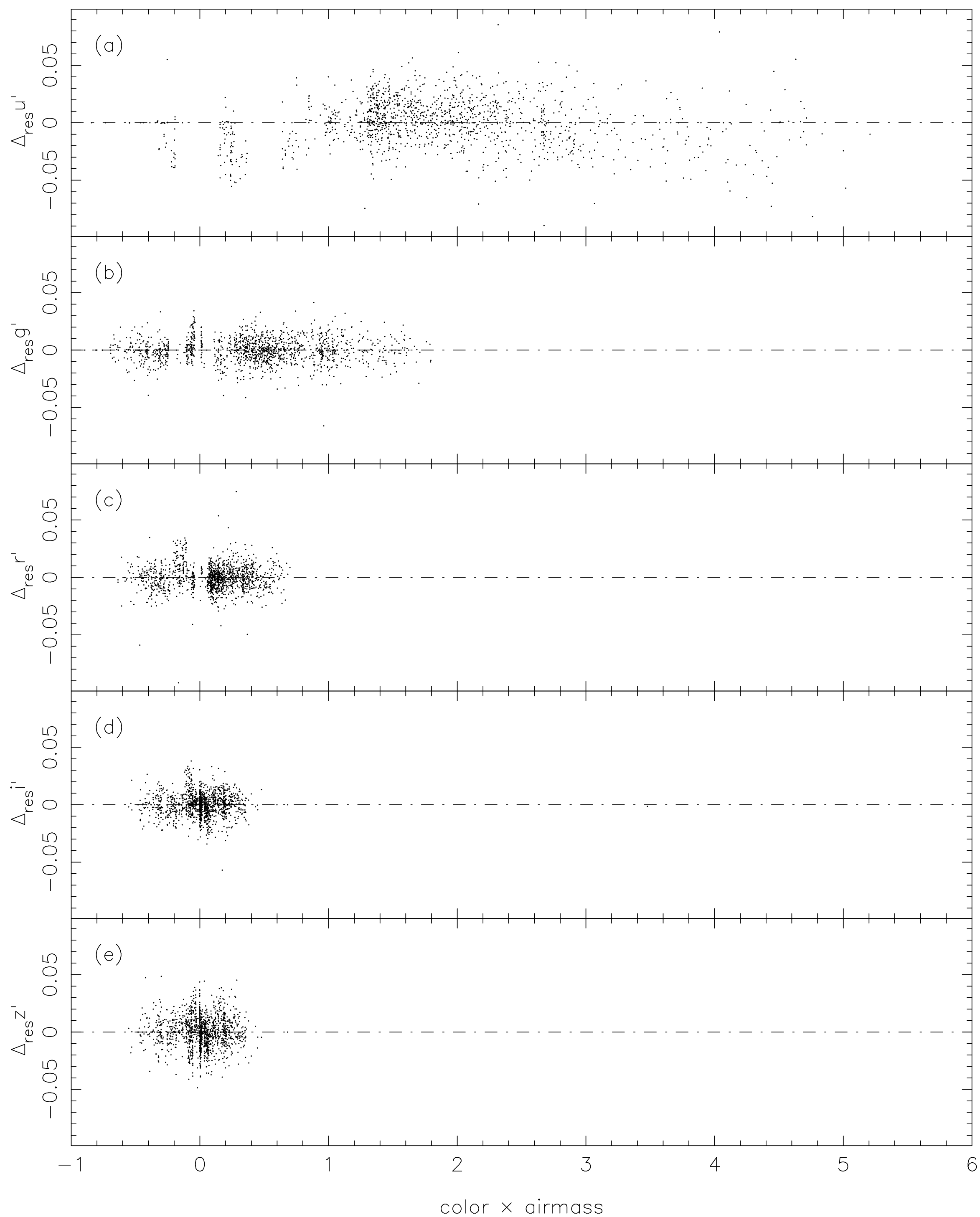

Fig. 12.— The residuals from the `excal` solutions for the Smith et al. (2002) standards plotted as a function of color×airmass for all the nights containing photometric data ($\Delta_{\rm res}u'$ vs. $(u'-g')\times X$, $\Delta_{\rm res}g'$ vs. $(g'-r')\times X$, $\Delta_{\rm res}r'$ vs. $(r'-i')\times X$, $\Delta_{\rm res}i'$ vs. $(i'-z')\times X$, $\Delta_{\rm res}z'$ vs. $(i'-z')\times X$).

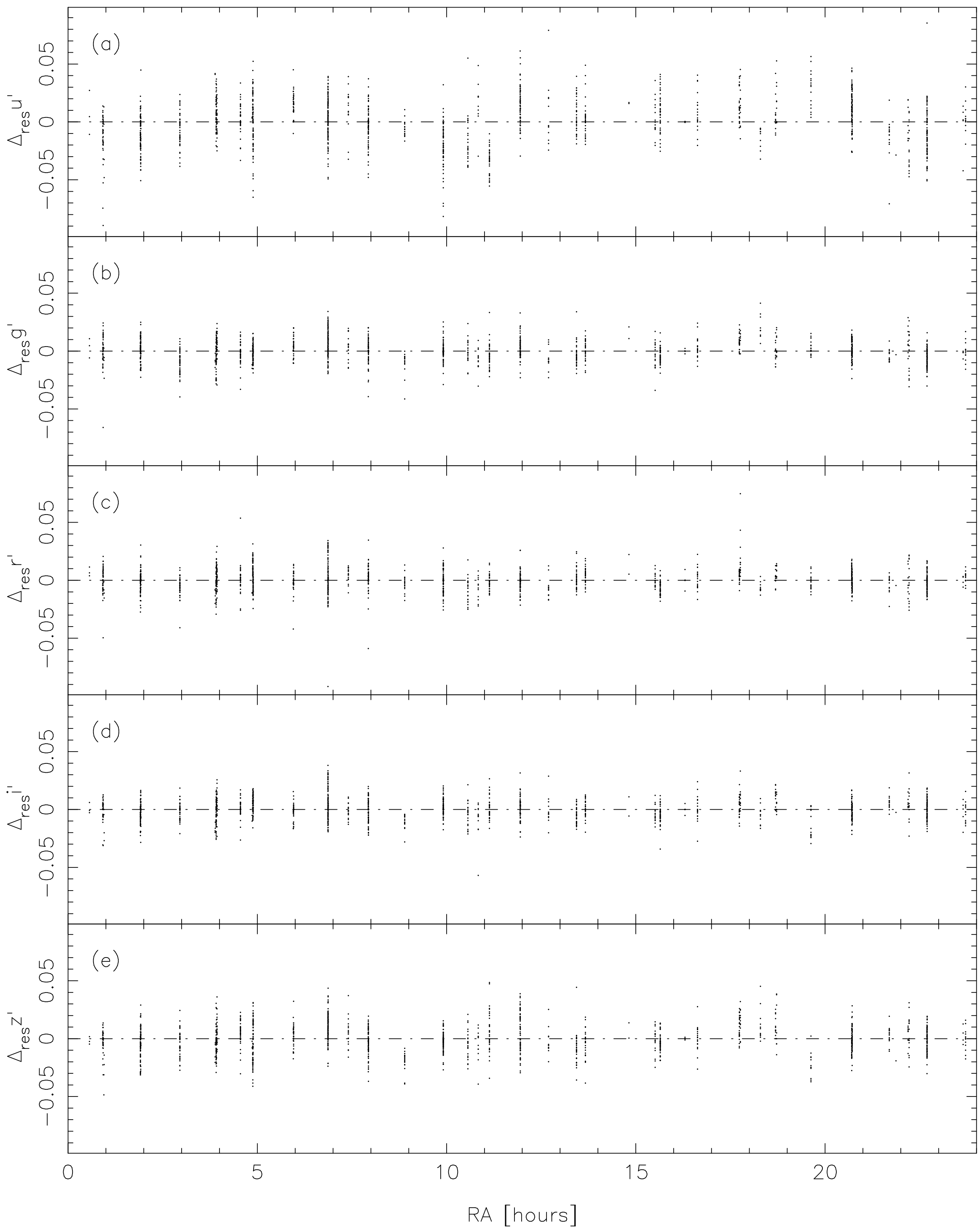

Fig. 13.— The residuals from the `excal` solutions for the Smith et al. (2002) standards plotted as a function of right ascension (RA) for all the nights containing photometric data.

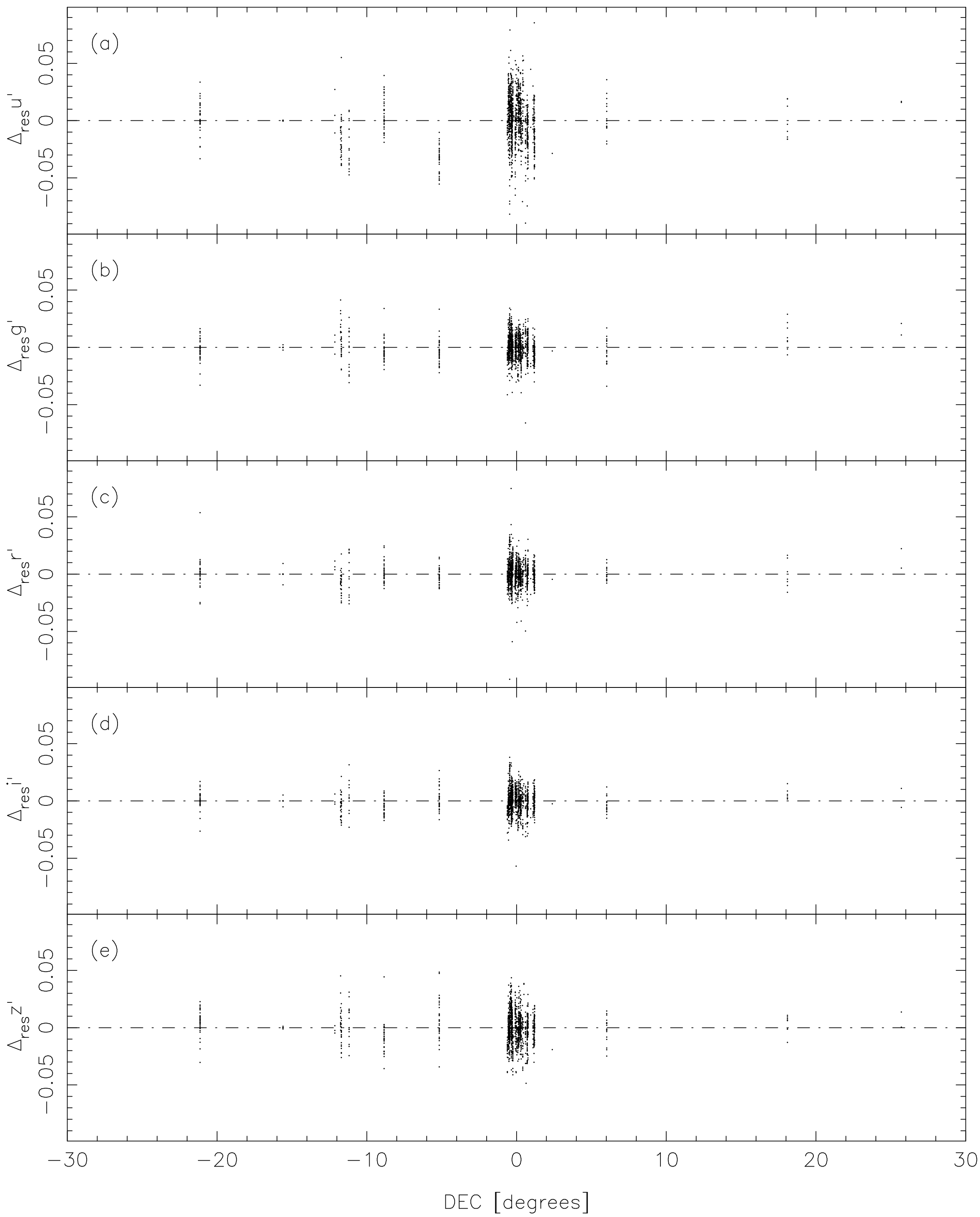

Fig. 14.— The residuals from the `excal` solutions for the Smith et al. (2002) standards plotted as a function of declination (DEC) for all the nights containing photometric data.

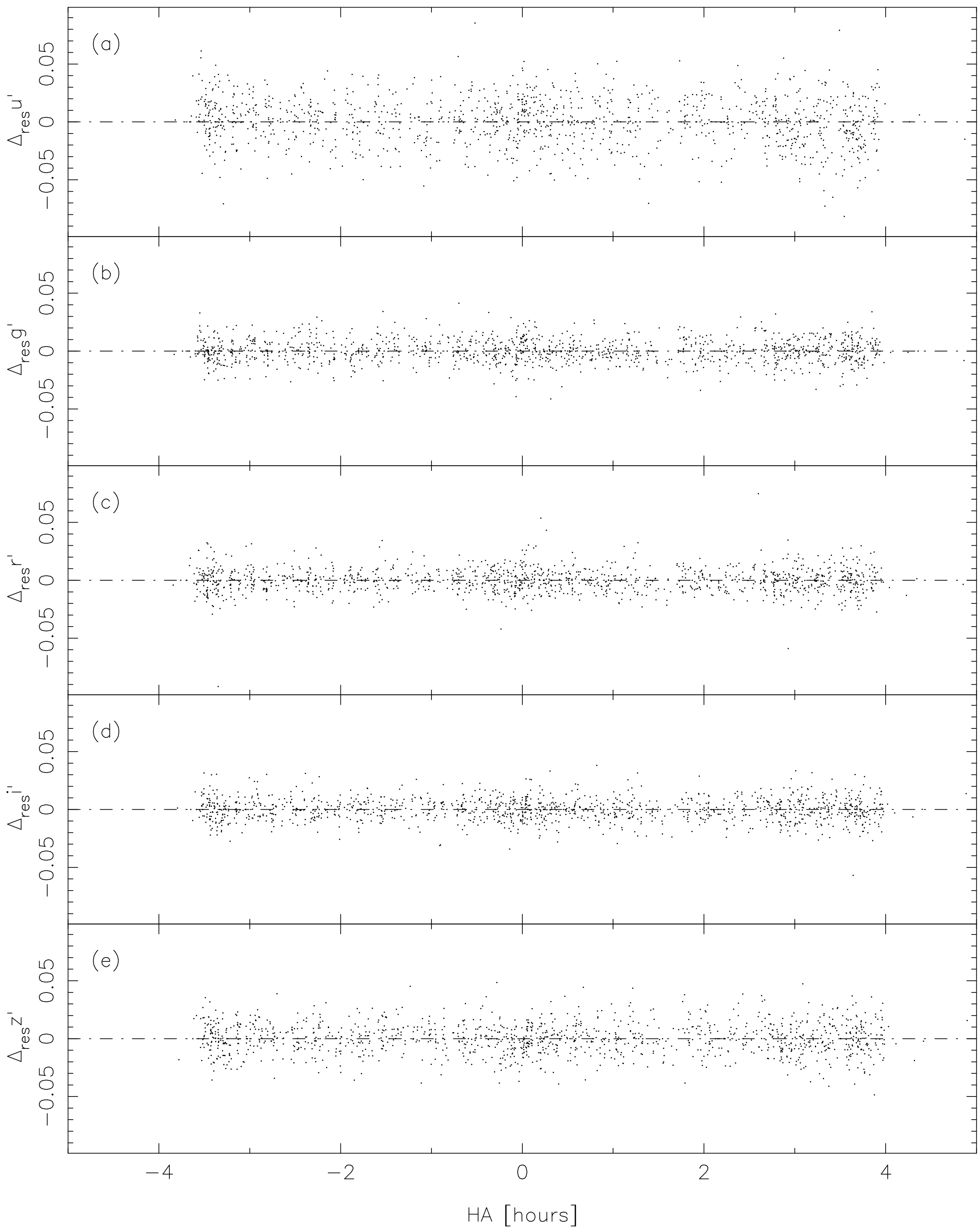

Fig. 15.— The residuals from the `excal` solutions for the Smith et al. (2002) standards plotted as a function of hour angle (HA) for all the nights containing photometric data.

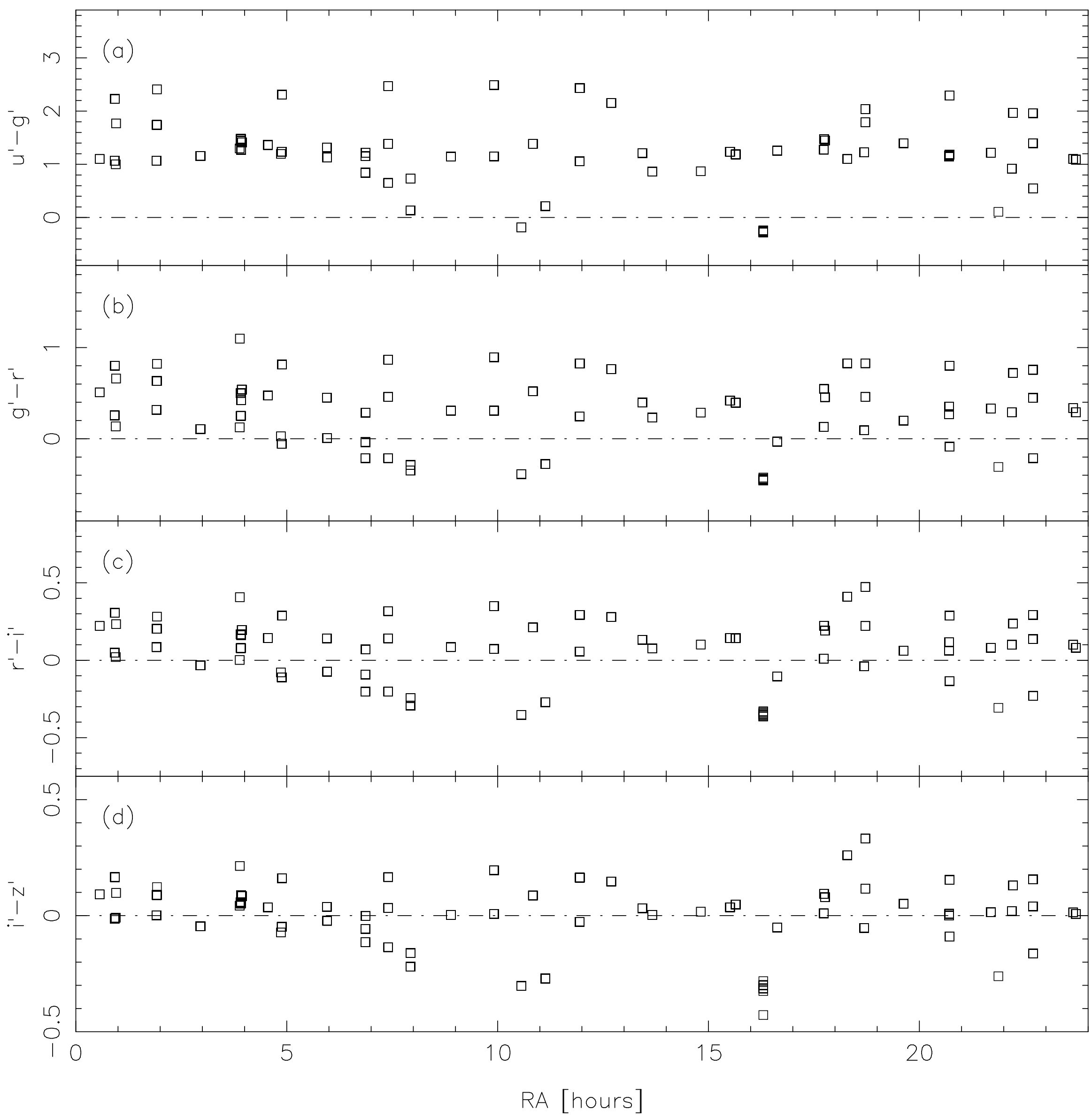

Fig. 16.— Color vs. right ascension of the Smith et al. (2002) standard stars used in the `excal` solutions for the Southern $u'g'r'i'z'$ standards program.

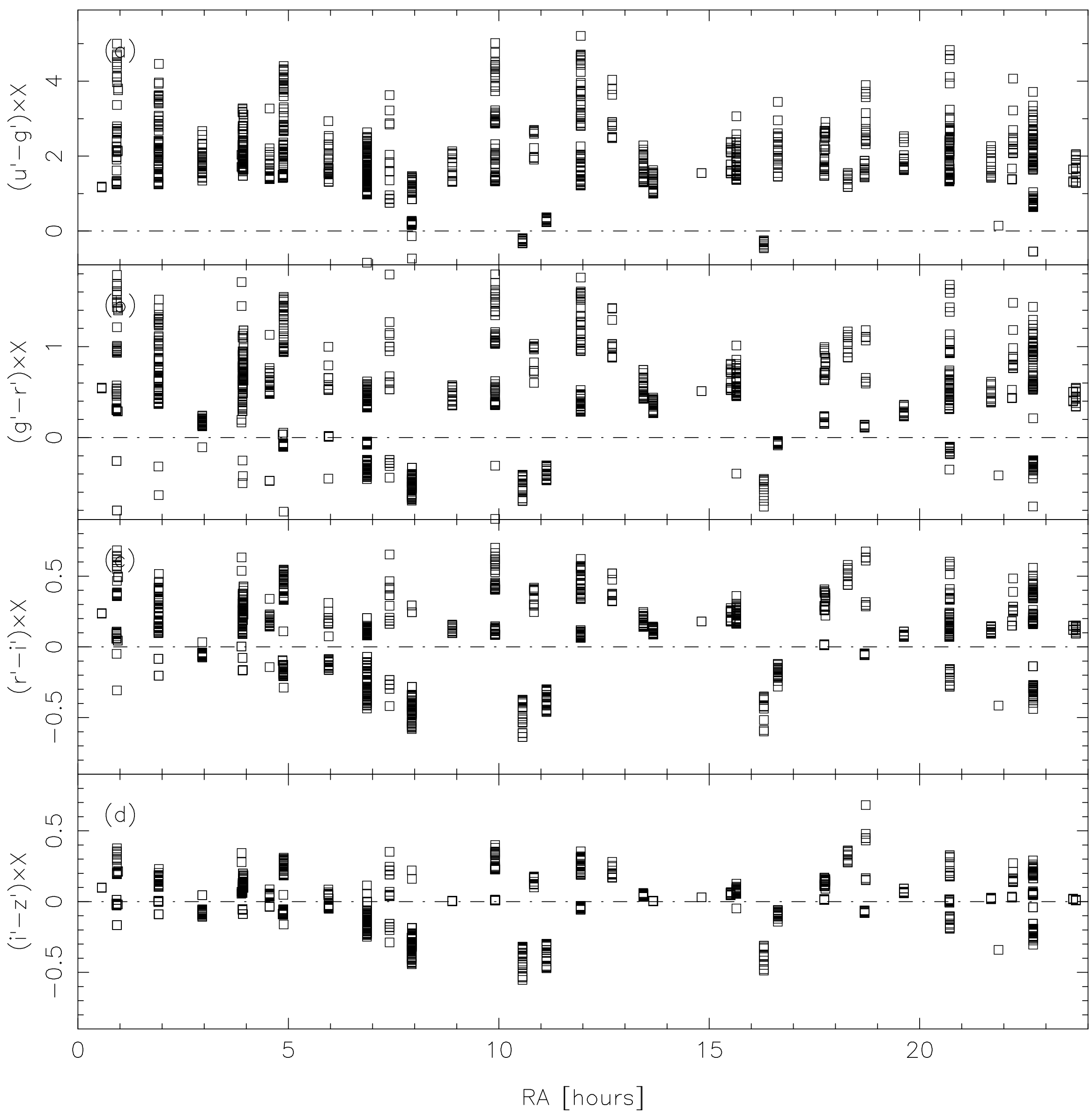

Fig. 17.— Color×airmass vs. right ascension of the Smith et al. (2002) standard stars used in the `excal` solutions for the Southern $u'g'r'i'z'$ standards program.

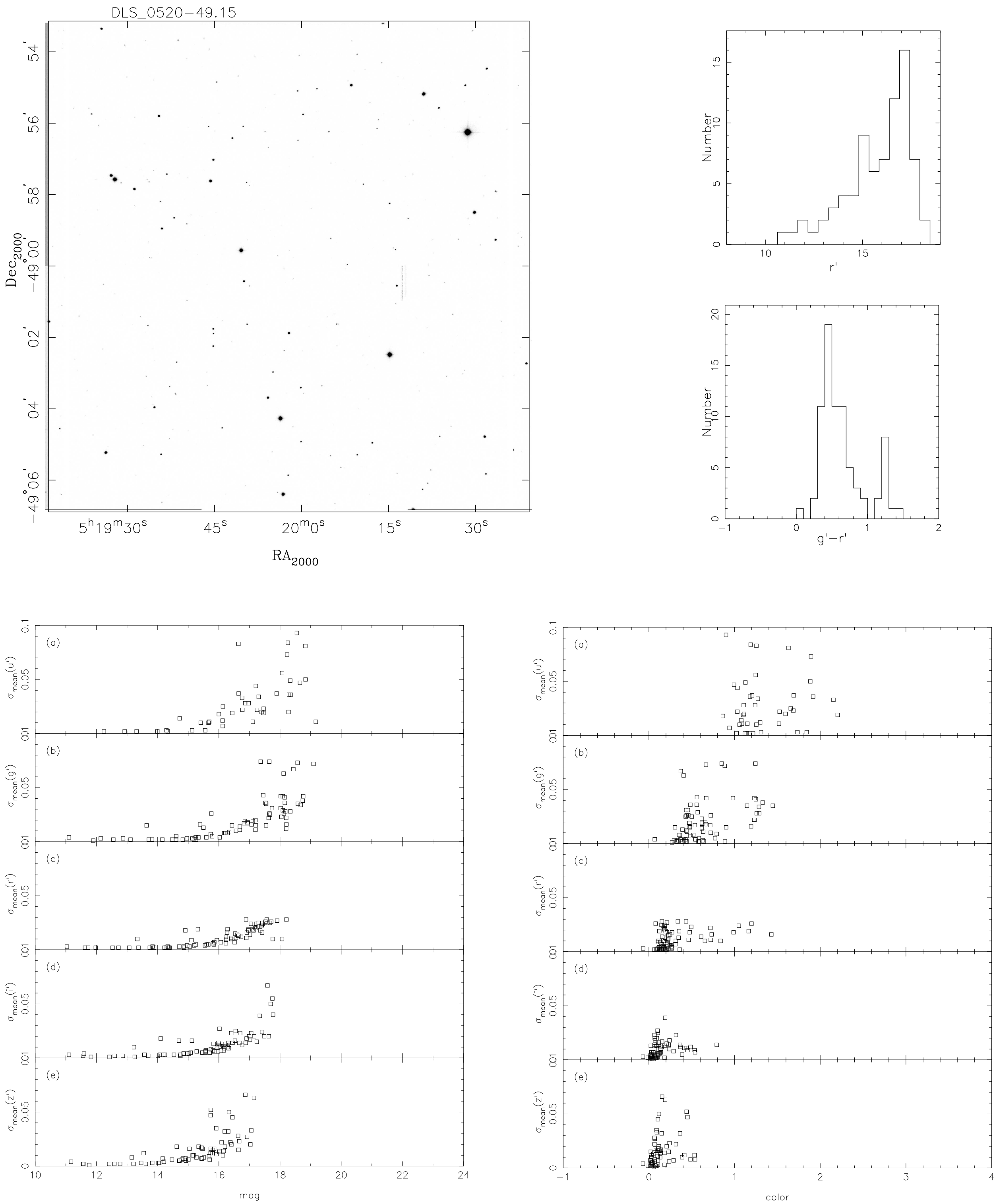

Fig. 18.— Example of a field's graphical summary page (in this case, for the field DLS_0520-49). This page includes an r'-band image for field verification, magnitude and color histograms for the standards in the field, and magnitude and color rms uncertainty plots for the standards.

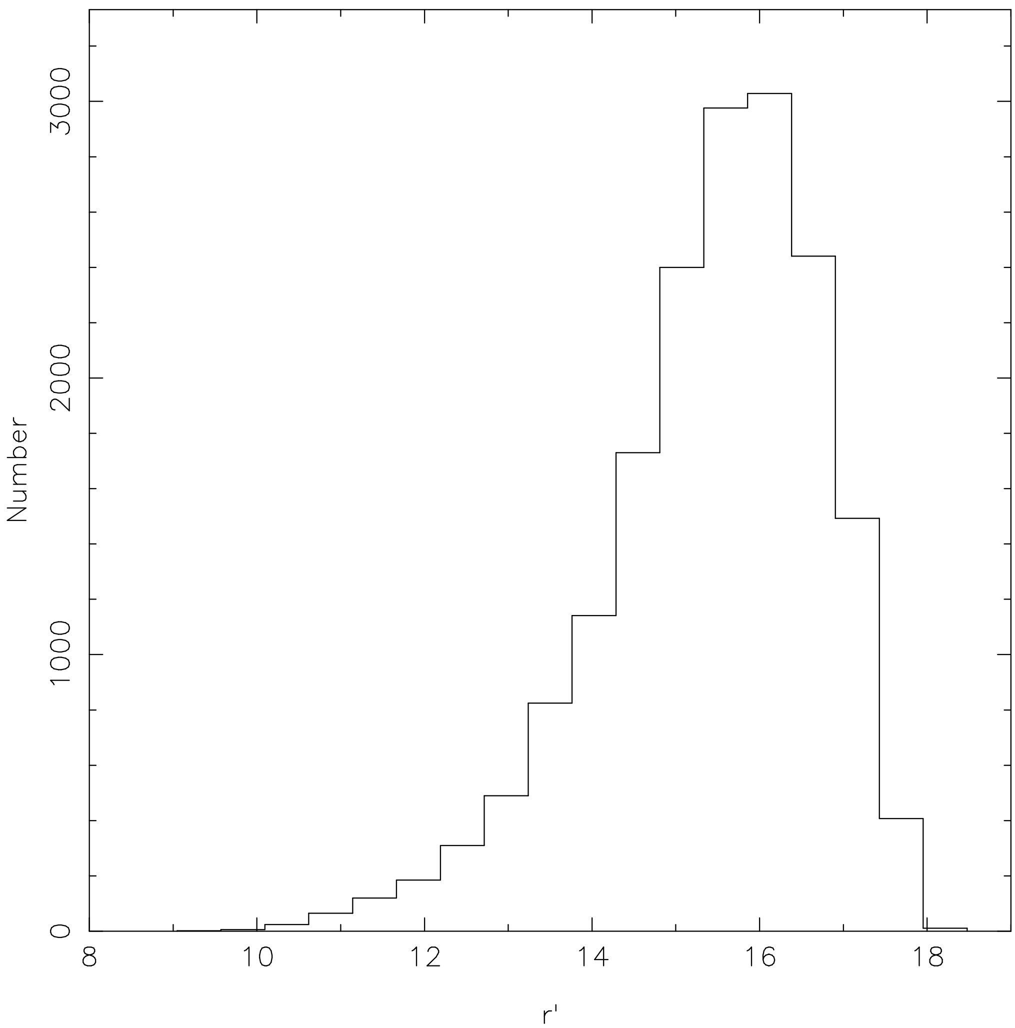

Fig. 19a.— Histogram of the distribution of stars by r' band magnitude. The faint end shows the effect of varying exposure times for the different fields. Each field finder chart has a similar plot to aid in selection while observing.

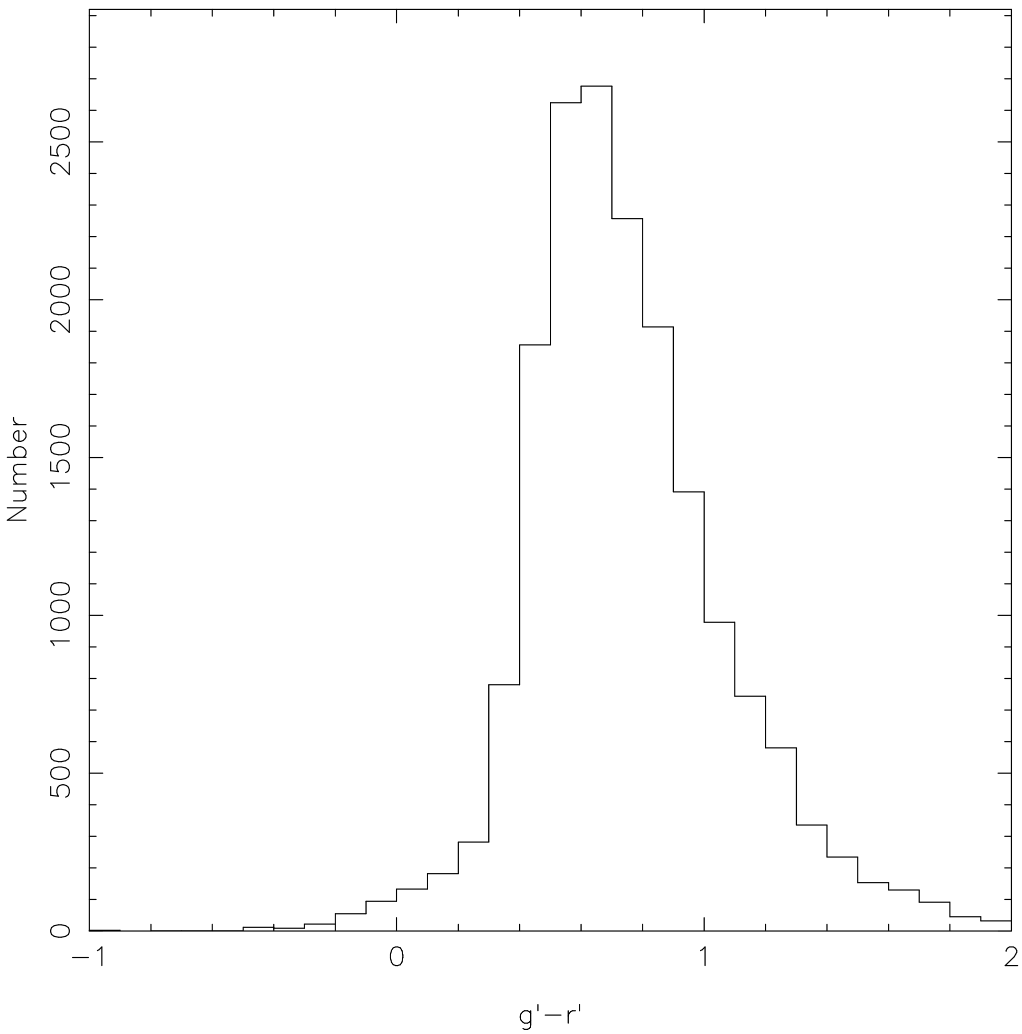

Fig. 19b.— Histogram of the distribution of stars by $(g' - r')$ color. This shows the color distribution of the network of standards. Each field finder chart has a similar plot to aid in selection while observing.

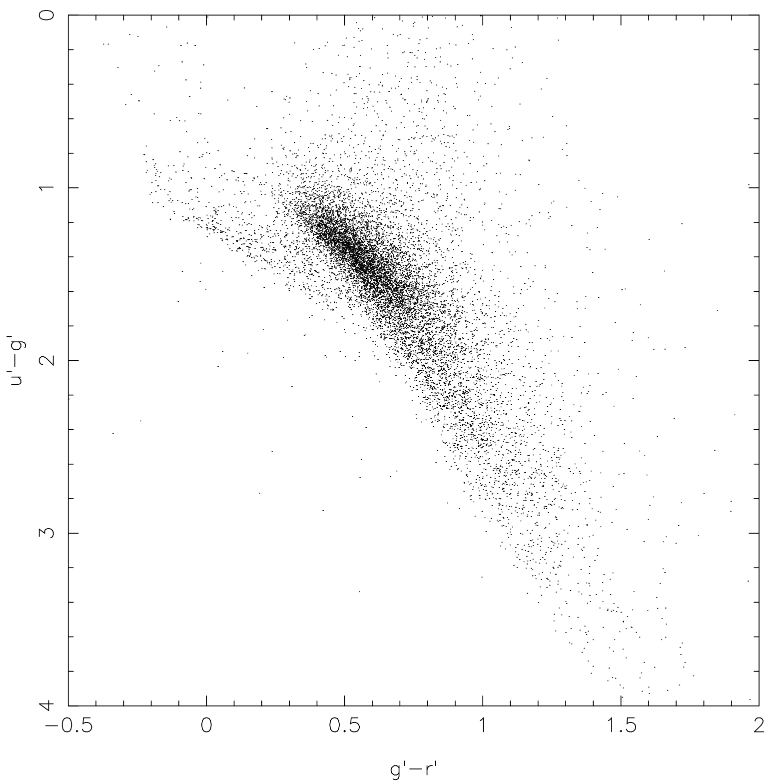

Fig. 20a.— The $(u' - g')$ vs. $(g' - r')$ color-color plot for the standard stars.

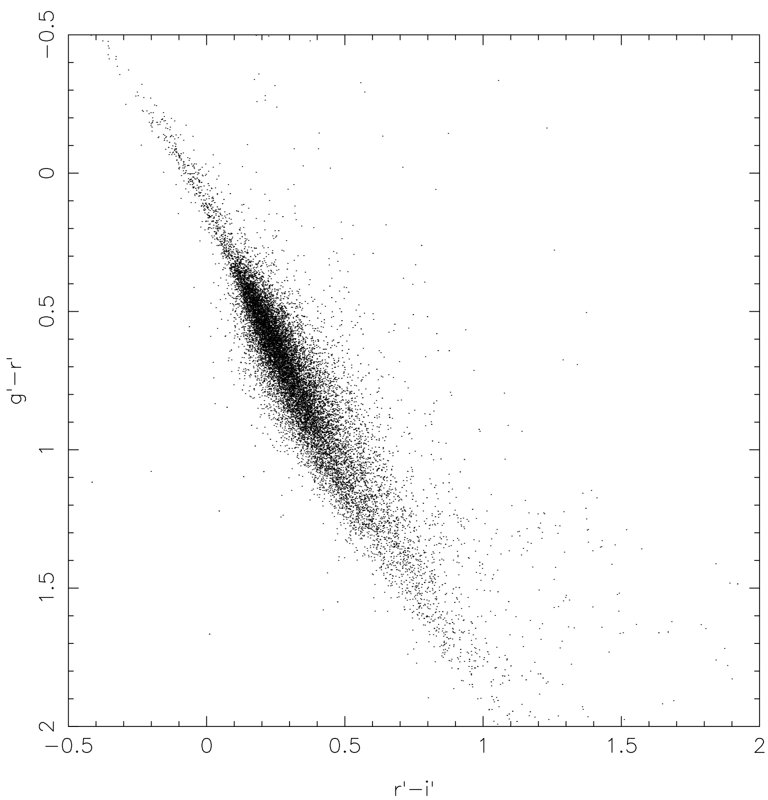

Fig. 20b.— The $(g' - r')$ vs. $(r' - i')$ color-color plot for the standard stars.

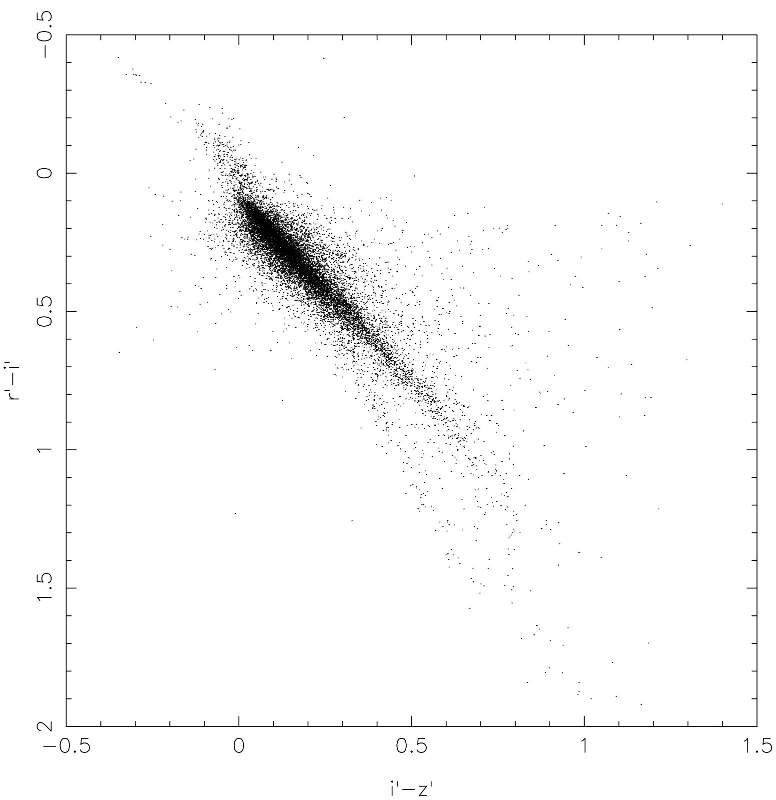

Fig. 20c.— The $(r' - i')$ vs. $(i' - z')$ color-color plot for the standard stars.